Redox Biology 37 (2020) 101609

Contents lists available at ScienceDirect

Redox Biology

journal homepage: www.elsevier.com/locate/redox

Bone marrow deficiency of mRNA decaying protein Tristetraprolin increases inflammation and mitochondrial ROS but reduces hepatic lipoprotein production in LDLR knockout mice

Fatma Saaoud[a,e], Junfeng Wang[a], Stephen Iwanowycz[a], Yuzhen Wang[a], Diego Altomare[b], Ying Shao[e], Jianguo Liu[c], Perry J. Blackshear[d], Susan M. Lessner[a], E. Angela Murphy[f], Hong Wang[g], Xiaofeng Yang[e,g,*], Daping Fan[a,**]

[a] Department of Cell Biology and Anatomy, University of South Carolina School of Medicine, Columbia, SC, 29209, USA
[b] Department of Drug Discovery and Biomedical Sciences, College of Pharmacy, University of South Carolina, Columbia, SC, 29208, USA
[c] Division of Infectious Diseases, Allergy and Immunology, Department of Internal Medicine, Saint Louis University School of Medicine, St. Louis, MO, 63104, USA
[d] Signal Transduction Laboratory, National Institute of Environmental Health Sciences, Research Triangle Park, NC, 27709, USA
[e] Centers for Inflammation, Translational & Clinical Lung Research, Departments of Microbiology and Immunology and Pharmacology, Lewis Katz School of Medicine, Temple University, Philadelphia, PA, 14190, USA
[f] Department of Pathology, Microbiology and Immunology, University of South Carolina School of Medicine, Columbia, SC, 29209, USA
[g] Metabolic Disease Research, Cardiovascular Research, and Thrombosis Research, Departments of Microbiology and Immunology, and Pharmacology, Lewis Katz School of Medicine, Temple University, Philadelphia, PA, 14190, USA

ARTICLE INFO

Keywords:
Tristetraprolin
Lipid metabolism
Lipoprotein
Inflammation
Atherosclerosis
Hepatic steatosis
Bone marrow transplantation (BMT)
Mitochondrial oxidative stress

ABSTRACT

Tristetraprolin (TTP), an mRNA binding and decaying protein, plays a significant role in controlling inflammation by decaying mRNAs encoding inflammatory cytokines such as TNFalpha. We aimed to test a hypothesis that TTP in bone marrow (BM) cells regulates atherogenesis by modulating inflammation and lipid metabolism through the modulation of oxidative stress pathways by TTP target genes. In a BM transplantation study, lethally irradiated atherogenic LDLR$^{-/-}$ mice were reconstituted with BM cells from either wild type (TTP$^{+/+}$) or TTP knockout (TTP$^{-/-}$) mice, and fed a Western diet for 12 weeks. We made the following observations: *(1)* TTP$^{-/-}$ BM recipients display a significantly higher systemic and multi-organ inflammation than TTP$^{+/+}$ BM recipients; *(2)* BM TTP deficiency modulates hepatic expression of genes, detected by microarray, involved in lipid metabolism, inflammatory responses, and oxidative stress; *(3)* TTP$^{-/-}$ BM derived macrophages increase production of mitochondrial reactive oxygen species (mtROS); *(4)* BM-TTP$^{-/-}$ mice display a significant reduction in serum VLDL/LDL levels, and attenuated hepatic steatosis compared to controls; and *(5)* Reduction of serum VLDL/LDL levels offsets the increased inflammation, resulting in no changes in atherosclerosis. These findings provide a novel mechanistic insight into the roles of TTP-mediated mRNA decay in bone marrow-derived cells in regulating systemic inflammation, oxidative stress, and liver VLDL/LDL biogenesis.

1. Introduction

Tristetraprolin (TTP), also known as mammalian Cth2 ortholog, Nup 475, TIS11, or G0S24, encoded by the Zinc Finger Protein-36 (*ZFP36*) gene, is an mRNA decaying protein containing tandem Cys-Cys-Cys-His (CCCH) zinc finger domain [1–3]. TTP has been reported to play important roles in the regulation of inflammation [4] and iron metabolism [3] by binding to the adenosine-uridine (AU) rich elements (AREs) in the 3' untranslated regions of its target mRNAs and leading to removal of their poly(A) tail and rapid degradation of the transcripts [5]. The majority of ARE-binding proteins promote the recruitment of ARE-containing mRNAs to the exosomes for eventual degradation, although some, such as Hu antigen R (HuR) family members, act as mRNA stabilizing factors [6]. In pathophysiological conditions, many

* Corresponding author. Centers for Inflammation, Translational & Clinical Lung Research, Metabolic Disease Research and Cardiovascular Research, Lewis Katz School of Medicine, Temple University, Philadelphia, PA, 14190, USA.
** Corresponding author. Department of Cell Biology and Anatomy, University of South Carolina School of Medicine, 6439 Garners Ferry Road, Columbia, SC, 29209, USA.
E-mail addresses: xfyang@temple.edu (X. Yang), daping.fan@uscmed.sc.edu (D. Fan).

https://doi.org/10.1016/j.redox.2020.101609
Received 12 March 2020; Received in revised form 30 May 2020; Accepted 14 June 2020
Available online 17 June 2020
2213-2317/ © 2020 The Authors. Published by Elsevier B.V. This is an open access article under the CC BY-NC-ND license (http://creativecommons.org/licenses/by-nc-nd/4.0/).

targets of TTP have been identified including mRNAs encoding tumor necrosis factor alpha (TNFalpha) [5,7,8], granulocyte macrophage-colony stimulating factor (GM-CSF) [9], interleukin-2 (IL-2) [10], IL-3 [11], IL-10 [12], IL-12 [13], IL-33 [14], and interferon-γ (IFN-γ) [15]. Global TTP knockout mice display complex inflammatory phenotypes characterized by growth retardation, myeloid hyperplasia, dermatitis, conjunctivitis, and arthritis, due to excessive production of TNFalpha [8,16]. These inflammatory phenotypes are attenuated by TNFalpha antibody or TNFalpha-receptor deficiency [8,17]. Furthermore, TTP deficiency results in endothelial dysfunction associated with increased levels of reactive oxygen and nitrogen species, indicating an increased oxidative stress in the $TTP^{-/-}$ mice [18]. However, it remains unknown whether TTP in bone marrow (BM) cells plays any role in modulating inflammation, lipid metabolism, and the expression of oxidative regulators during atherogenesis.

Lipid metabolism dysregulation is involved in many pathologic conditions such as atherosclerotic cardiovascular diseases, which are the leading cause of morbidity and mortality worldwide [19]. Dyslipidemia and a chronic inflammatory state are key contributors to the development of atherosclerotic cardiovascular diseases. Unlike other chronic inflammatory diseases, the unique aspect of atherosclerosis is the significant roles that lipids and lipoprotein metabolism play. Atherosclerosis is characterized by the formation of atherosclerotic plaques in the arterial wall initiated with endothelial activation and dysfunction followed by sub-endothelial lipid accumulation, blood monocyte migration and their differentiation into macrophages, and foam cells formation [20–26]. There is accumulating evidence showing that lipids can directly affect inflammatory responses and vice versa, and the interactions between the inflammatory pathways and lipid components that initiate atherosclerosis have been extensively studied [27]. Current evidence supports the roles of inflammatory cells, a collection of various danger associated molecular patterns (DAMPs), especially lipid-derived DAMPs such as oxidized low density lipoprotein (oxLDL), and their interactions with each other in all phases of atherosclerosis [28,29]. The recent success of the CANTOS trial revealed that anti-human IL-1β antibody can reduce cardiovascular event rates and validated the concept that targeting inflammation can reduce atherosclerosis without affecting lipid levels [30]. In addition to lipid lowering, the anti-inflammatory effects of statins also have been considered responsible for their protective effects in patients with atherosclerotic cardiovascular diseases. The JUPITER study demonstrated that statins reduced cardiovascular risk in primary prevention, even in otherwise healthy individuals with elevated CRP levels [31]. Determination of the functional denominators that links lipid metabolism and immune/inflammation activation could facilitate the development of novel therapeutic strategies for cardiovascular diseases.

In this study, we transplanted BM cells from either $TTP^{-/-}$ or $TTP^{+/+}$ mice into lethally-irradiated atherogenic low density lipoprotein receptor knockout ($LDLR^{-/-}$) mice fed a Western-type diet. We aimed to evaluate whether inflammatory response and lipid metabolism are regulated by $TTP^{-/-}$ bone marrow-derived cells and can be a dominator to drive atherosclerosis, and to determine the underlying molecular mechanisms. Our results demonstrate that: 1) BM TTP deficiency resulted in increased systemic and multi-organ inflammation; 2) BM TTP deficiency significantly increased mitochondrial ROS production; 3) BM TTP deficiency modulated lipid metabolism-, and inflammation-related genes in the liver; 4) BM TTP deficiency dramatically reduced serum lipid levels, attenuated hepatic steatosis, and decreased fecal cholesterol excretion; and 5) increased inflammation and reduced lipids offset each other, resulting in unchanged atherosclerosis. Our results indicated for the first time that deficiency of a master mRNA-decay protein TTP in bone marrow-derived cells reduces VLDL/LDL levels, which offsets the enhanced inflammation in atherogenesis.

2. Materials and methods

2.1. Human carotid atherosclerotic specimens

In accordance with a protocol approved by the Institutional Review Board at the University of South Carolina, human carotid artery specimens were collected from de-identified carotid atherosclerotic patients undergoing carotid endarterectomy with patients' informed consent at Greenville Memorial Hospital (Greenville health system, Greenville, SC, USA) and Palmetto Hospital (Palmetto Health System, Columbia, SC, USA), which confirmed the Declaration of Helsinki. Specimens were sliced transversely into 7-mm segments. One segment from each specimen was dissected into separate samples representing atheromatous lesion and the surrounding normal media. Tissues were sonicated and lysed in Qiazol for RNA extraction. Quantitative real-time PCR (qRT-PCR) was used to measure the expression of human TTP.

2.2. Mice

Seven-week-old female $LDLR^{-/-}$ mice were obtained from Jackson Laboratories (Bar Harbor, Maine). Female TTP KO mice [8,16] and their wild-type littermates on a C57Bl/6 background at age of 8 weeks were used as bone marrow donors. All mice were kept under specific pathogen-free conditions in a temperature controlled environment at the University of South Carolina according to National Institutes of Health guidelines. Animal care and experiments were approved by the Institutional Animal Care and Use Committee at the University of South Carolina.

2.3. Bone marrow transplantation (BMT) and atherosclerosis induction in mice

Bone marrow cells from wild type ($TTP^{+/+}$) or TTP knockout ($TTP^{-/-}$) donor mice were harvested by flushing cleaned femurs and tibias with sterile RPMI-1640 media (Invitrogen Life Technologies, Grand Island, NY, USA). The cell suspension was centrifuged at $300 \times g$ for 5 min and re-suspended in ice-cold phosphate buffer saline (PBS). $LDLR^{-/-}$ mice received autoclaved water supplemented with 100 mg/L neomycin and 500,000 U/L polymyxin B sulfate one week before till two weeks after BMT. Recipient mice were lethally irradiated with a single dose of 9 Gy using a cesium gamma source. Four hours (h) later, 5×10^6 BM cells (in 200 μl PBS) from donor mice were administered by retro-orbital injection into the irradiated mice. To assess the irradiation efficiency, two mice that did not receive BM cells after irradiation were used as controls; they died within 2 weeks after irradiation while all the BM transplanted mice survived. After 4 weeks of recovery, the chimeric mice were fed a Western-type diet for 12 weeks to induce atherosclerosis. The Western-type diet contains 21% anhydrous milkfat, 34% sucrose, and 0.2% cholesterol (Diet 3 TD.88137; Harlan Laboratories, Indianapolis, IN). During the Western-type diet-feeding period, body weight and food intake were assessed weekly. At the experimental endpoint, chimeric mice were euthanized; and venous blood from the retro-orbital venous plexus puncture was collected into heparinized tubes for assessment of cell counts, blood glucose, and lipid profile. Tissues including hearts, aortic roots, liver, spleen and lung were collected and analyzed as described below.

2.4. Peritoneal macrophage isolation and culture

A standard procedure was used to isolate thioglycollate-elicited peritoneal macrophages. Briefly, mice were injected intraperitoneally (i.p.) with 3 mL of 3% (w/v) sterile thioglycollate (BD Biosciences Clontech; Palo Alto CA). After three days, peritoneal macrophages were collected by washing the peritoneal cavity twice with 10 ml cold PBS. Cells were centrifuged at $300 \times g$ for 5 min, resuspended and cultured in Dulbecco's modified Eagle's medium (DMEM, Invitrogen, Grand Island,

NY) supplemented with 10% fetal bovine serum (FBS) and a combination of 1% penicillin/streptomycin (Sigma-Aldrich, St. Louis, MO, USA), and 50 μM of β-mercaptoethanol. Two hours later, cells were washed with PBS to remove the non-adherent cells; the adherent macrophages were cultured in serum free DMED media (SFM) overnight at 37 °C and 5% CO_2. Macrophages were then stimulated with 50 ng/ml lipopolysaccharide (LPS, Sigma-Aldrich) for 6 h under the same conditions. Cells were then lysed with Trizol reagent (Invitrogen, Grand Island, NY) for RNA extraction. Expression of pro-inflammatory cytokines TNFalpha and IL-6 was detected by qRT-PCR.

2.5. Bone marrow-derived macrophage (BMDM) isolation and culture

BMDMs were isolated and cultured as previously described [32]. Briefly, femurs and tibias were isolated from BM-TTP deficient and littermate control mice. BM cells were flushed out using 10 ml of RPMI medium with a 27-gauge needle. Single-cell suspensions of bone marrow precursors were centrifuged, resuspended in RPMI medium containing 30% L929 cell-conditioned medium as a source of M-CSF and cultured in 6-well plates for seven days for further experiments.

2.6. Total RNA extraction, cDNA synthesis, and quantitative real-time PCR

Total RNAs were isolated from cultured macrophages and liver tissue using an RNeasy Mini kit (Qiagen, Germantown, MD) and following the manufacturer's instructions. One microgram of isolated RNA of each sample was reverse transcribed into cDNA using an iScript™ cDNA synthesis kit (Bio-Rad, Hercules, CA). qRT-PCR was performed on a Bio-Rad CFX96 system (Bio-Rad, Hercules, CA) using iQ™ SYBR® Green Supermix (Bio-Rad) according to the manufacturer's instructions. The relative expression of target mRNA was calculated using the $2^{(-\Delta\Delta Ct)}$ method by normalizing target mRNA Ct values to those of the housekeeping gene, 18s RNA. PCR thermal cycling conditions consisted of 3 min at 95 °C, and 40 cycles of 15 s at 95 °C and 58 s at 60 °C. Samples were run in triplicate. Primers used are listed in Supplemental Table S1.

2.7. VetScan hematology analysis

Blood was drawn into heparinized tubes by retro-orbital puncture. Blood samples were run on the VetScan HMT hematology analyzer (Abaxis, Union City, CA). The following parameters were measured: total red blood cells (RBC), hemoglobin, mean corpuscular hemoglobin (MCH), mean corpuscular hemoglobin concentration (MCHC), hematocrit (Hct), platelet number, mean platelet volume (MPV), platelet distribution width (PDW), total white blood cells (WBC), lymphocytes, mean cell volume (MCV), and red cell distribution width (RDW).

2.8. Blood glucose measurement

Blood glucose levels were detected using OneTouch Ultra Blood Glucose Monitoring System (LifeScan, Inc., Milpitas, CA) following the manufacturer's instructions.

2.9. Plasma lipid and lipoprotein analysis

Serum total cholesterol (TC) and triglyceride (TG) levels were determined using enzymatic colorimetric assays with Cholesterol Reagent and Triglycerides GPO reagent kits (Raichem; San Diego, CA) following the manufacturer's instructions, and analyzed by Soft-Max Pro5 software (Molecular Devices, Sunnyvale CA). In brief, mice were anesthetized with isoflurane; blood was collected by retro-orbital venous plexus puncture, and plasma was obtained via centrifugation at 4000 × *g* for 20 min. Serum was diluted 1:100 in sterile water, 100 μL of diluted serum and 100 μL of freshly prepared cholesterol and triglyceride reagent were added to each microplate well. The plates were incubated for 10 min at 37 °C and the absorbance was measured at 540 nm. Plasma lipoprotein profile was measured using a fast performance liquid chromatography (FPLC) system (AKTA purifier, GE Healthcare Biosciences, Pittsburgh, PA) equipped with a Superose 6 10/300 GL column (GE Healthcare). Pooled mouse serum (100 μL) was loaded onto the column, and eluted at a constant flow rate of 0.5 mL/min with 1 mM sodium EDTA and 0.15 M NaCI. Fractions of 0.5 mL were collected and the cholesterol concentration from each fraction was measured.

2.10. Flow cytometry analysis

The spleen was removed from freshly euthanized mice and smashed in 10 mL RPMI-1640 medium supplemented with 10% FBS using Stomacher® 80 Biomaster (Seward Laboratory Systems Inc., Port St. Lucie, FL). To obtain single cell suspensions, tissues were passed through a 70-μm cell strainer. After red blood cell (RBC) lysis, cells were stained with anti-CD19 mAb, anti-CD3 PE mAb, anti-CD4 FITC mAb, anti-CD8a FITC mAb, anti-FOXP3 mAb, anti-ly6C FITC mAb, anti-CD11b PE mAb, anti-ly6G FITC mAb, and/or anti F4/80 FITC mAb (eBioscience, San Diego, CA) on ice for 30 min. For mitochondrial ROS measurement, BMDM were cultured in 6-well plate. On day 7, cells were stimulated with H_2O_2 (250 μM) for 4 h. After staining with MitoSOX Red Mitochondrial Superoxide indicator (5 μM) (Life technologies, Carlsbad, CA), cells were incubated at 37 °C for 20 min and washed with PBS twice. Cells were detached by adding 1 ml accutase (Innovative Cell Technologies, Inc) for 30 min, collected by centrifugation, and resuspended in 0.2 ml FACS buffer. Stained cells were subjected to flow cytometry analysis using a Cytomics FC 500 flow cytometer and CXP software version 2.2 (Beckman coulter, Brea, CA). Data were collected for 10,000 live events per sample.

2.11. Enzyme-linked immunosorbent assay (ELISA)

ELISA assays were performed per the manufacturer's protocol (eBiosciences). Briefly, blood was collected and centrifuged at 4000 × *g* for 20 min. The serum layer was removed and diluted 1:5. Each well in 96-well ELISA plates was coated with 100 μL of TNFalpha capture antibody (2 μg/mL) and the plates were incubated overnight at 4 °C. The cells were incubated with 300 μL of blocking solution (1% BSA, 5% sucrose, and 0.05% NaN3) for 1 h at room temperature. Next, 100 μL of each sample were loaded in each well and incubated for 2 h at room temperature. After washing three times, the plates were incubated with biotinylated anti-mouse TNFalpha (250 ng/mL), 1 μg/mL horseradish peroxidase streptavidin and substrate solution. The reaction was stopped by adding 50 μL of 1 M H_2SO_4 solution. Recombinant mouse TNFalpha was used to generate a linear standard curve. Optical density was determined with a SpectraMax M5 microplate reader at 450 nm (Molecular Devices). All samples were tested in triplicate.

2.12. Atherosclerosis analysis

At the experimental endpoint, all mice were euthanized; and the vasculature was perfused with cold 1x PBS. Aortic roots were isolated and embedded in Optimal Cutting Temperature (OCT; Tissue-tek) compound (Sakura Finetek, Inc., Torrance, CA) in a plastic mold and stored at −20 °C. Cryosections (10-μm thick) were cut from the proximal 1 mm of the aortic root. Aortic root sections were assessed for atherosclerotic plaque size following Hematoxylin and Eosin staining. To analyze the accumulation of macrophages in the atherosclerotic plaque, Moma-2 (Abcam, Cambridge, MA) staining was performed. Sections were fixed in acetone for 20 min at room temperature, rinsed with PBS, followed by blocking in immunostain blocker solution, and then rinsed with PBS again. The endogenous peroxidase activity was blocked with 3% hydrogen peroxide. Sections were blocked for non-specific staining with 5% normal goat serum for 30 min at room

temperature followed by incubation with Moma-2 primary antibody at 4 °C overnight. After washing with PBS for three times, the biotinylated goat anti-rabbit IgG (Vector Laboratories, Burlingame, CA) was used as the secondary antibody. Immunoreactivity was amplified using the Vectastain ABC kit (Vector Laboratories), and the signal was enhanced by peroxidase enhancer (GeneTex, Irvine, CA) and reacted with the substrate from AEC Chromogen/FRP substrate kit (GeneTex Irvine, CA). Nuclei and cytoplasm were counterstained with hematoxylin for 1 min. Finally, sections were washed with deionized water and air-dried before the addition of coverslips. Macrophage infiltration was analyzed via microscope. Oil red-O staining was performed to detect lipid content in atherosclerotic plaques. Slides were placed in oil red-O (Sigma-Aldrich) working solution (0.5% in 100% propylene glycol) for 4 h at room temperature. Slides were then placed in 85% aqueous propylene glycol for 1 min. This step was repeated 3 times. Slides were then rinsed with deionized water for 2 min. Sections were stained with aqueous hematoxylin (GeneTex, Irvine, CA; USA) for 20 s. Slides were further washed with deionized water and air-dried. Sections were covered with cover glasses and analyzed under a microscope. Plaque collagen content was analyzed using Masson's trichrome staining. Slides were fixed in Bouin's fluid for 1 h at 60 °C, washed with distilled water, and then placed in Working Weigert's Iron Hematoxylin Stain for 10 min. Sections were stained with Biebrich Scarlet-acid Fuchsin solution for 15 min and rinsed in distilled water. Next, sections were placed in Phosphotungstic-Phosphomolybdic Acid solution for 10 min, and then placed in Aniline blue for 5 min followed by 1% Acetic Acid solution for 3 min. Finally, slides were dehydrated and cleared through 95% ethanol, 100% ethanol, and xylenes, 2 changes each, mounted with permount, and cover-slipped. All images were recorded with a Nikon E600 Wide field Epifluorescence microscope and Micropublisher digital camera with Q-imaging software. Plaque size, lipid content, collagen percentage, and macrophage cell content were quantified by computerized image Pro-Plus.

2.13. Histological analysis

Tissue samples including liver, lung, and spleen were fixed in 10% neutral buffered formalin and processed according to standard protocols before being stained with hematoxylin-eosin. All tissue sections were visualized with a Nikon E 600 microscope.

2.14. Microarray analysis

Total RNA was extracted from liver tissue using RNeasy Mini kit (Qiagen, Germantown, MD). RNA quality and quantity analysis were determined using an Agilent 2100 Bioanalyzer. All RNA samples had an RNA integrity number (RIN) of 9.2 or higher. The RNA was amplified and labeled with the Agilent Low Input Quick Amp labeling kit according to the manufacturer's instructions. Then, RNA was transcribed into cDNA using a poly-dT primer that also contained the T7 RNA polymerase promoter sequence. Subsequently, T7 RNA polymerase was added to cDNA samples to amplify the original mRNA molecules and to simultaneously incorporate cyanine-3 labeled CTP into the amplification product (cRNA). Labeled cRNA molecules were purified using Qiagen's RNeasy Mini Kit (Valencia, CA). After spectrophotometric assessment of dye incorporation and cRNA yield, samples were hybridized to Agilent whole mouse genome microarrays 8 × 60,000 using a gene expression hybridization kit (Agilent) according to the manufacturer's recommendation. Microarray analysis was performed using an Agilent DNA microarray scanner system. After washes, arrays were scanned using a High Resolution Agilent DNA Microarray Scanner and images saved in tagged image file format (TIFF). A heat map of genes was generated using R function heatmap.2.

2.15. Statistical analyses

Statistical analysis was performed with GraphPad Prism 6.0 software (GraphPad Software Inc, San Diego, CA). Data are presented as mean ± standard error of the mean (SEM). Normal probability plot or Kolmogorov–Smirnov test was performed for both groups of data to ensure the validity of normality assumption. Statistical significance was determined by two-tailed Student *t*-test for two-group comparison. Data were considered statistically significant at $p < 0.05$.

3. Results

3.1. TTP is up-regulated in human carotid atherosclerotic lesions

TTP has been shown to be expressed at very low levels in unstimulated human aortic endothelial cells (HAECS); but after LPS stimulation its expression levels are significantly increased [33]. Moreover, TTP expression levels are significantly increased in purified monocytes and macrophages isolated from human carotid atherosclerotic lesions compared to the macrophages isolated from alveolar lavage of healthy subjects [34]. However, TTP expression levels in atherosclerotic lesions compared to non-lesion area for the same patient have not been examined. We used qRT-PCR to measure human TTP mRNA expression levels from 12 atherosclerotic patients. Atherosclerotic lesions and the surrounding normal tissue were isolated from human carotid arteries from patients undergoing carotid endarterectomy (CEA). Our data show that delta Ct values were slightly, but statistically significantly, reduced in the atheroma lesions. Since delta Ct values are inversely related to the TTP gene expression levels, reduced delta Ct values indicate upregulation of TTP expression in carotid atherosclerotic lesions compared to the surrounding normal carotid tissue from the same patient (Supplemental Fig. S1). These results suggest that TTP may play a regulatory role during the atherogenic process.

3.2. Bone marrow TTP deficiency reduces body weight of BM recipient LDLR$^{-/-}$ mice

Lethally irradiated LDLR$^{-/-}$ mice were transplanted with BM cells from TTP$^{-/-}$ or TTP$^{+/+}$ mice. After 4 weeks of recovery, the chimeric mice were challenged with a Western diet for 12 weeks, after which animals were euthanized for collection of tissues (Fig. 1A). During the Western diet-feeding period, body weight and food intake were measured weekly. None of the mice showed any signs or symptoms of bone marrow transplantation rejection. We did not observe a significant difference in food intake between groups (Fig. 1B). There was, however, a reduction in the body weight in BM-TTP$^{-/-}$ mice (Fig. 1C). Of note, body weight reduction was reported to be the most important phenotypic feature of whole body TTP knockout mice [8], suggesting a regulatory role for TTP from bone marrow-derived cells in metabolic processes.

3.3. Bone marrow TTP deficiency increases neutrophil granulocytes and platelets in peripheral blood

Previous reports showed that TTP knockout mice develop a hematological and immunological disturbance [8,35,36]. To detect the hematological effects of TTP deficiency in BM cells on atherogenic LDLR$^{-/-}$ mice fed a Western diet; we performed a Vetscan HMT analysis of peripheral blood. Our results show that BM TTP deficiency significantly increased numbers and percentages of neutrophils (Fig. 2A and B). Additionally, total platelet numbers and platelet hematocrit were significantly increased in BM-TTP$^{-/-}$ mice (Fig. 2C and D). On the other hand, blood monocyte, lymphocyte (Supplemental Fig. S2A), and red blood cell counts, hemoglobin concentration, hematocrit, mean corpuscular volume, mean corpuscular hemoglobin, MCHC, and RDWC

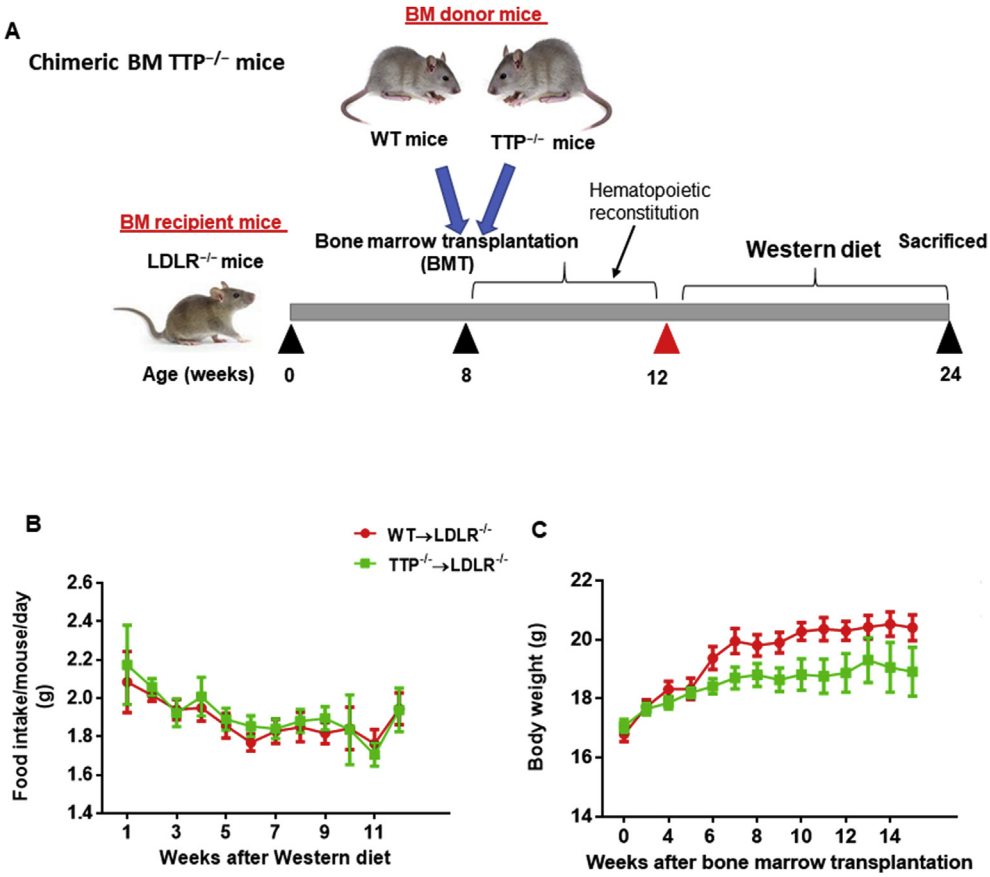

Fig. 1. Bone marrow TTP deficiency did not affect food intake but reduced body weight of BM recipient LDLR$^{-/-}$ mice. (A) Schematic representation of TTP$^{-/-}$ bone marrow transplantation (BMT). Eight week-old female LDLR$^{-/-}$ mice were transplanted with TTP$^{-/-}$ or TTP$^{+/+}$ bone marrow cells. Four weeks after BMT, mice were fed a Western diet for 12 weeks. During the Western diet period, mouse body weight and food intake were measured weekly. (B) Food intake and (C) Growth curves of the mice. The average daily intake of Western diet per mouse was calculated (N = 9 mice per group). Data were presented as mean ± SEM.

were not different between the groups (Supplemental Fig. S2B).

Flow cytometry analysis of the leukocyte populations in the spleen showed a significant increase in CD11b^{+}/GR1^{+} cells, CD11b^{+}/Ly6G^{+} neutrophils, and CD11b^{+}/Ly6C^{high} inflammatory monocytes in the BM-TTP$^{-/-}$ mice. The number and percentage of CD19^{+} B-lymphocytes, CD3^{+}/CD8a^{+} T-lymphocytes, CD4^{+}/FoxP3^{+} T-cells, CD4^{+}/IL17^{+} cells, CD11C^{+} cells, F4/80^{+} cells, and CD11b^{+}/Ly6C^{low} cells were comparable between the two groups (Fig. 2E and F). Even though the spleens of BM-TTP$^{-/-}$ mice were slightly enlarged (Supplemental Fig. S2C), the absolute cell numbers were comparable between the two groups (Supplemental Fig. S2D). These data suggest that TTP deficiency in bone marrow-derived cells results in select hematopoietic and immunological disturbances.

3.4. TTP deficiency macrophages express pro-inflammatory cytokines at increased level

Stimulated macrophages produce a variety of pro-inflammatory cytokines and chemokines such as TNFalpha and IL6. These cytokines/chemokines play a crucial role in the macrophage response to lipopolysaccharide (LPS) stimulation [37,38]. Macrophages isolated from Rag2$^{-/-}$ mice transplanted with TTP-deficient BM cells over-secreted TNFalpha upon LPS stimulation, which is associated with increased TNFalpha mRNA levels in the cells [35]. The mechanism underlying increased TNFalpha synthesis and secretion has been attributed to stabilization of TNFalpha mRNA in the absence of TTP [7]. Thus, we hypothesized that BM TTP deficiency of LDLR$^{-/-}$ mice will increase TNFalpha production upon LPS stimulation. We isolated thioglycollate-elicited peritoneal macrophages from BM-TTP$^{-/-}$ mice and control mice. Macrophages were then cultured and stimulated with LPS (50 ng/ml) for 6 h. The expressions of pro-inflammatory cytokine TNFalpha and IL6 mRNA were measured. Our results show that TNFalpha mRNA expression levels (Fig. 3A) were significantly increased in TTP$^{-/-}$ macrophages after LPS stimulation, whereas, IL6 mRNA levels were slightly but not significantly increased (Fig. 3B) compared to TTP$^{+/+}$ macrophages. These data indicated that TTP deficient peritoneal macrophages have a higher ability to produce TNFalpha after LPS stimulation than controls, suggesting that TNFalpha is likely one of the pathophysiological targets for TTP-mediated RNA degradation, consistent with a previous report [8].

3.5. Bone marrow TTP deficiency increases inflammation

It has been reported that global TTP$^{-/-}$ mice develop severe inflammatory syndrome associated with cachexia, arthritis, conjunctivitis, dermatitis, myeloid hyperplasia, splenomegaly, and autoimmunity [8]. To examine if BM-TTP$^{-/-}$ mice have a comparable inflammatory phenotype, we collected tissues from BM-TTP$^{-/-}$ mice and stained with hematoxylin and eosin to examine inflammatory cell infiltration. BM-TTP$^{-/-}$ mice showed more inflammatory cell infiltration than the control mice. LDLR$^{-/-}$ mice transplanted with TTP$^{-/-}$ BM cells had a comparable liver weight to LDLR$^{-/-}$ mice transplanted with wild type BM cells (Supplemental Fig. S3). However, BM-TTP$^{-/-}$ mice had significantly increased inflammatory cell infiltration in the liver compared to BM-TTP$^{+/+}$ mice (Fig. 3C). Similarly, lungs of BM-TTP$^{-/-}$ mice had more inflammatory cell infiltration surrounding the vasculature, indicating the increased movement and migration of inflammatory cells. In addition, these mice exhibited more inflammatory exudate in the alveolar space compared to the control group (Fig. 3D). The spleen showed loss of normal organization with no clear demarcation between the red and the white pulp due to inflammatory cell infiltration (Fig. 3E).

To further define the effects of BM TTP deficiency on systemic inflammation in LDLR$^{-/-}$ mice, we performed ELISA analyses to measure serum TNFalpha levels. Indeed, our data show that BM TTP deficiency significantly increased serum TNFalpha concentration in

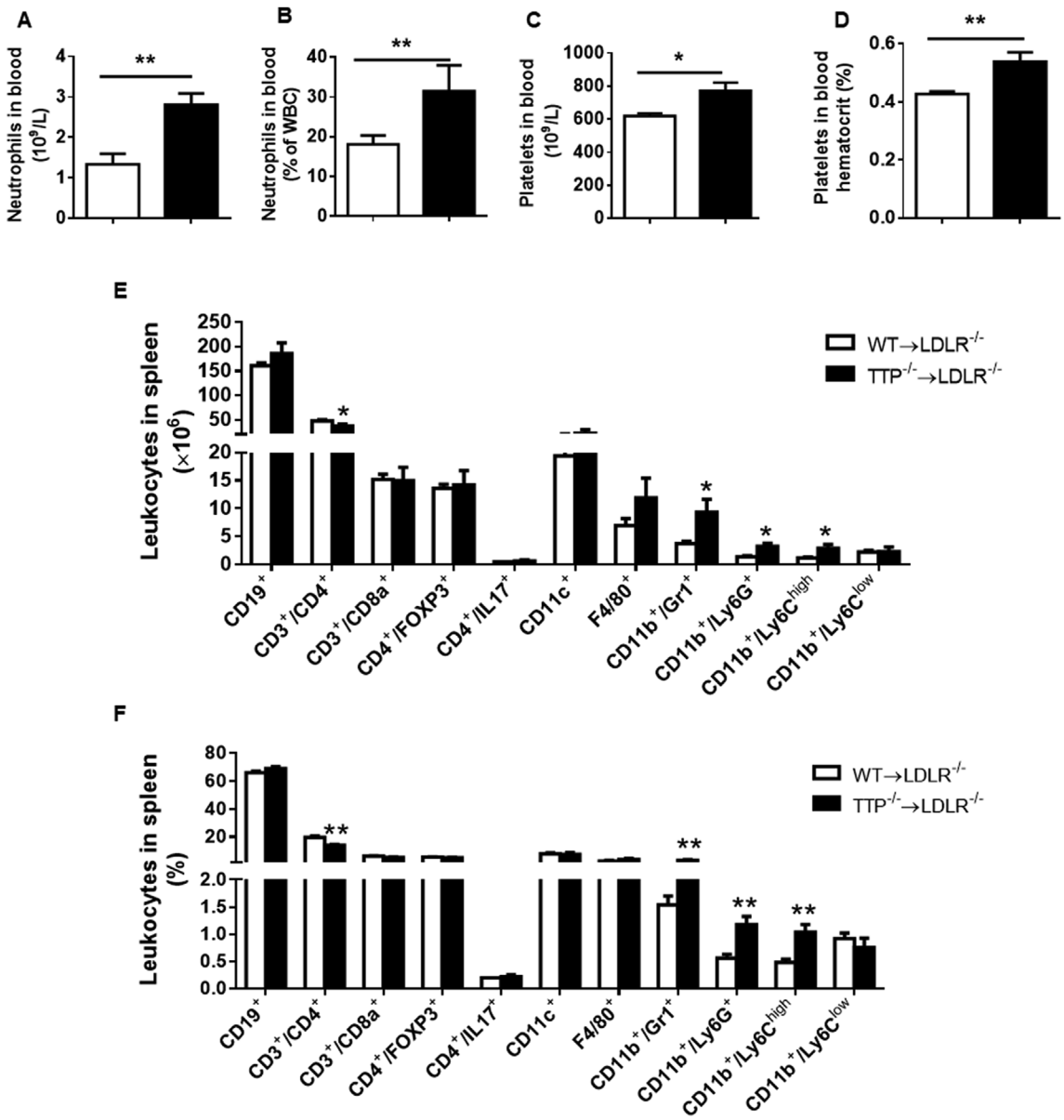

Fig. 2. Bone marrow TTP deficiency increased neutrophil granulocytes, platelets in peripheral blood, and inflammatory monocytes in the spleen. At the experimental endpoint, peripheral blood was drawn into heparinized tubes by retro-orbital puncture. Blood samples were run on the VetScan HMT hematology analyzer to measure the following parameters: (A, B) Neutrophil granulocyte numbers and percentages; (C, D) Total platelet numbers and platelet hematocrit. (E, F) Flow cytometry analysis of mouse splenocytes. A single cell suspension was made, and cells were stained with anti-CD19 mAb, anti-CD3 PE mAb, anti-CD4 FITC mAb, anti-CD8a FITC mAb, anti-FOXP3 mAb, anti-ly6C FITC mAb, anti-CD11b PE mAb, anti-ly6G FITC mAb, and anti F4/80 FITC mAb to detect different mouse leukocyte populations. Absolute numbers (A) and percentages (B) of various leukocyte subpopulations in the spleen. All data were presented as the mean ± SEM (N = 6 mice each group). *P < 0.05; **P < 0.01, vs WT BM recipient group.

LDLR$^{-/-}$ mice (Fig. 3F). Taken together, our results indicate that BM TTP deficiency significantly increases systemic and multi-organ inflammation in LDLR$^{-/-}$ mice.

3.6. Bone marrow TTP deficiency modulates the expression of liver genes involved in inflammation and lipid metabolism

The liver plays a significant role in lipid and lipoprotein metabolism including lipid biosynthesis and lipoprotein production and secretion. Lipid accumulation in hepatocytes results in hepatic steatosis, which may develop as a consequence of multiple dysfunctions such as alterations in very low density lipoprotein (VLDL) secretion and fatty acid synthesis pathways. Impaired hepatic lipid metabolism is tightly correlated with obesity, diabetes, non-alcoholic fatty liver disease, and atherosclerotic cardiovascular diseases [39–41]. Hyperlipidemia has been shown to associate with systemic inflammation; and inflammatory responses can affect lipid accumulation and vice versa [42,43]. Both hyperlipidemia and chronic inflammation are recognized as major driving forces in atherogenesis [20]. To access the expression levels of hepatic genes related to lipid metabolism and inflammation in atherogenic LDLR$^{-/-}$ mice transplanted with TTP$^{-/-}$ BM cells, a microarray gene analysis was performed on mRNAs isolated from liver tissue of BM-TTP$^{-/-}$ and BM-TTP$^{+/+}$ mice. Using a corrected P-value cut-off of 0.05 and an absolute fold change of > 2.00 we found that BM TTP deficiency in LDLR$^{-/-}$ mice significantly modulated 236 genes (Fig. 4A and Supplemental Fig. S6). To identify the functional pathways in the liver that were altered by BM TTP deficiency, we analyzed the 236 genes using Ingenuity Pathway Analysis (IPA) software. We then

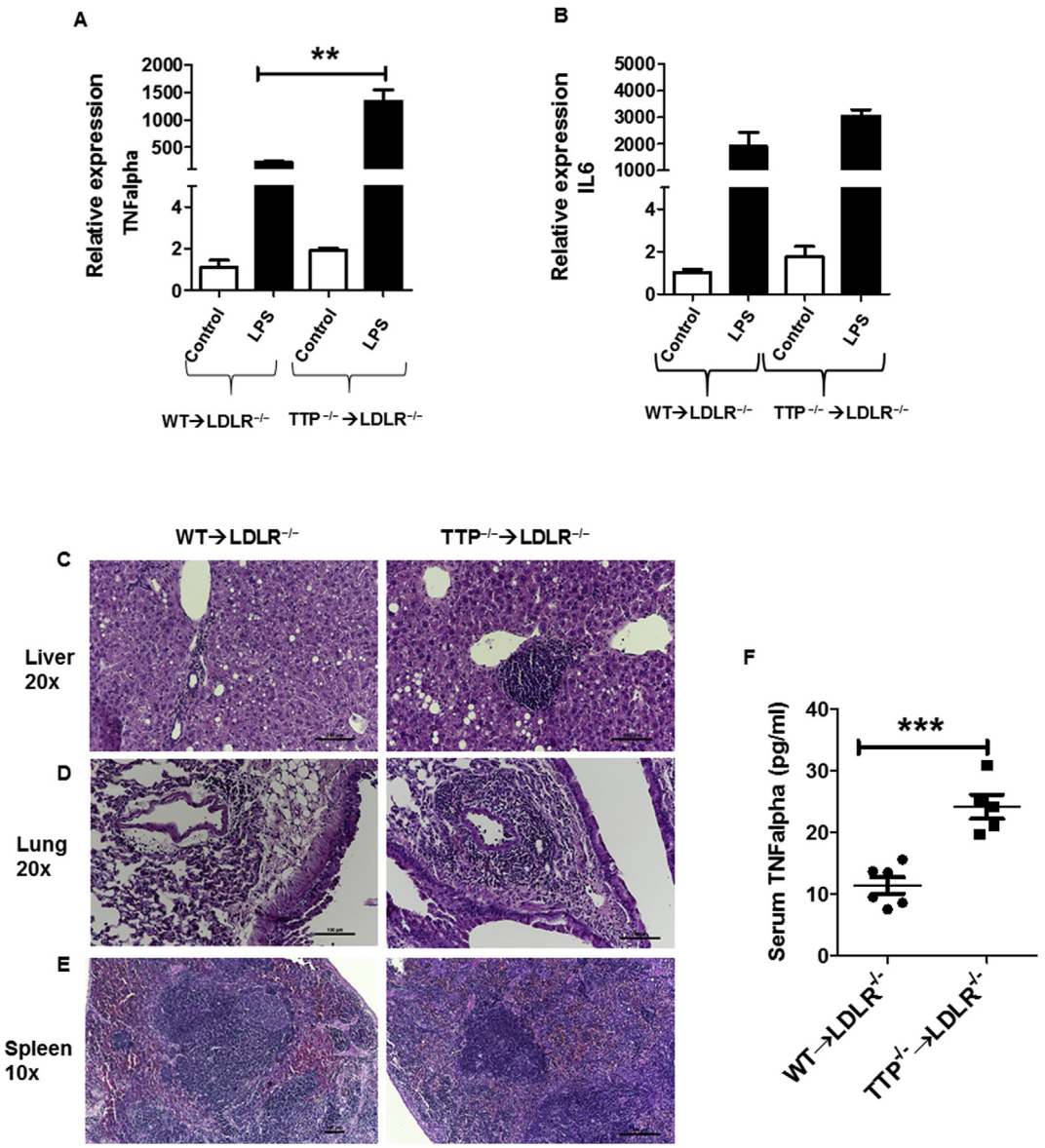

Fig. 3. Bone marrow TTP deficiency increased macrophage response to LPS stimulation, and resulted in multi-organ damage and systemic inflammation. (A–B) Residential peritoneal macrophages were obtained from mice at the experimental endpoint. The cells were treated with LPS (50 ng/ml) for 6 h. Total mRNA was extracted for qRT-PCR to measure the expression of inflammatory cytokine TNFalpha (A) and IL6 (B). Data were expressed as mean ± SEM, (N = 3 mice for each group). **$p < 0.01$. Representative photomicrographs showing H&E staining in the (C) liver (20x), (D) lung (20x), and (E) spleen (10x) in wild-type recipient mice (right panels) and $TTP^{-/-}$ recipient mice (left panels). Scale bar 100 μm. (F) Serum TNFalpha concentrations were determined by ELISA. Data were analyzed by Student's *t*-test. Data were presented as the mean ± SEM (N = 6 mice each group). ***$p < 0.001$.

examined top molecular pathways that were regulated by BM TTP deficiency, "Inflammatory response" and "Fatty acid metabolism". Of the 236 genes, 27 genes involved in lipid metabolism and inflammatory response were identified as being significantly changed with BM TTP deficiency (Fig. 4B). Interestingly, sterol regulatory element binding transcription factor 1 (SREBF1), which controls the expression of enzymes involved in fatty acid and cholesterol biosynthesis, was significantly downregulated; whereas serum amyloid A1 (SAA1) and C–C chemokine receptor type 2 (CCR2), which are inflammatory response related genes, were highly expressed in the liver of BM-$TTP^{-/-}$ mice (Fig. 4C and D).

To confirm the gene expression patterns identified by the microarray analysis, we performed qRT-PCR analysis for select genes. The results show that mRNA expression levels were in agreement with the microarray data. Notably, SREBF1 expression level was significantly reduced whereas the expression levels of the inflammatory genes CCR2 and SAA1 were significantly increased in the liver of $LDLR^{-/-}$ mice transplanted with $TTP^{-/-}$ BM cells (Fig. 4E).

Taken together, our data indicated that multiple key genes related to lipid metabolism and inflammation are influenced by BM TTP deficiency, suggesting that TTP deficiency in BM cells could change the hepatic expression of genes of lipid metabolism and inflammation.

3.7. Bone marrow TTP deficiency increases mitochondrial ROS production

Reactive oxygen species (ROS), by-products in various metabolic pathways have the potential to damage cellular macromolecules including DNA, proteins, and lipids [44]. The majority of ROS are produced by the mitochondrial respiratory reactions indicating that mitochondrial respiratory proteins play pivotal roles in the regulation of oxidative stress [45]. Mitochondrial ROS (mtROS) can increase pro-inflammatory cytokines production and promote development of

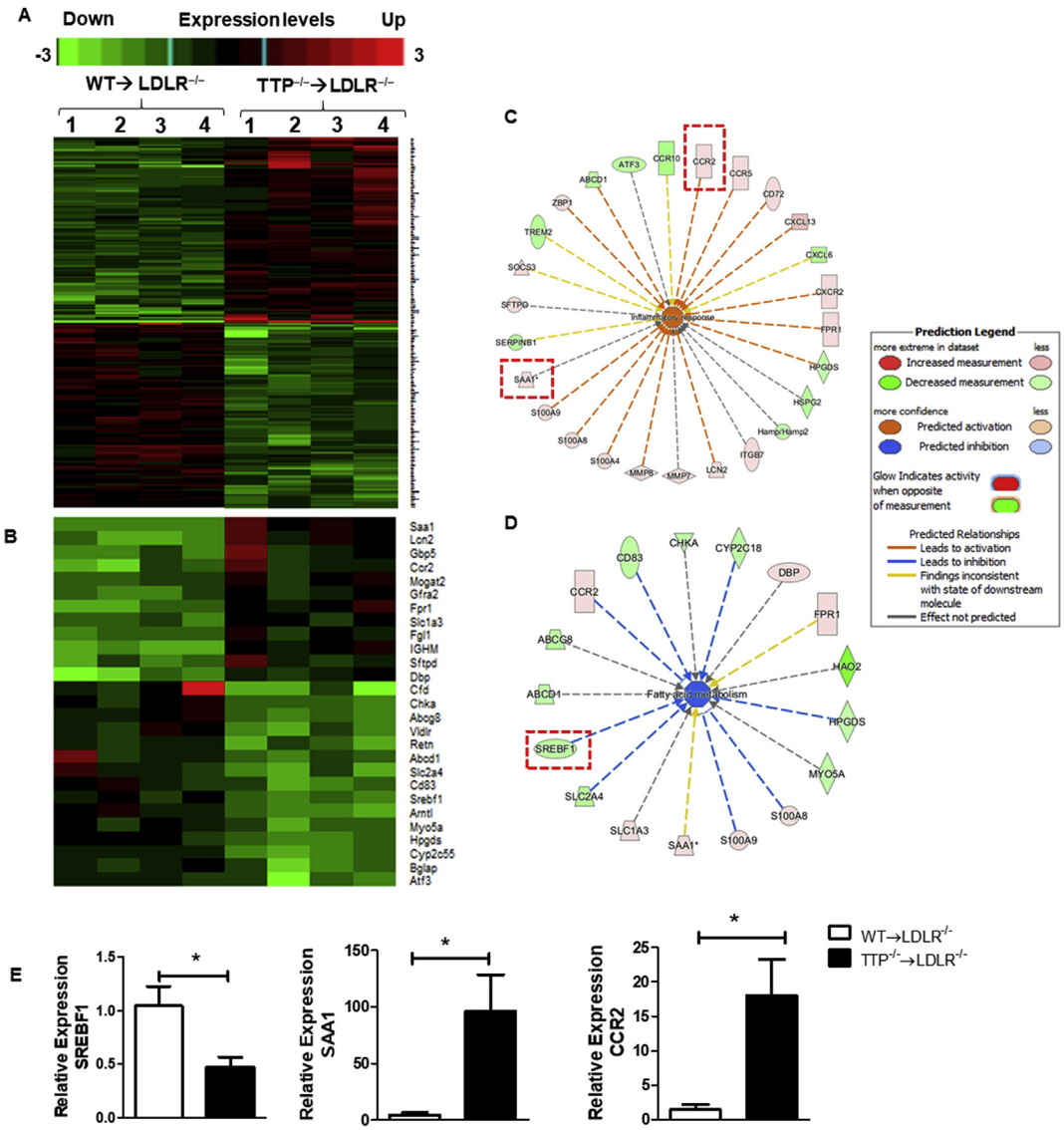

Fig. 4. Microarray analysis revealed that bone marrow TTP deficiency in LDLR$^{-/-}$ mice modulated the expression of inflammatory genes, oxidative stress regulators, and lipid metabolism related genes. Mouse liver RNAs were isolated from LDLR$^{-/-}$ mice transplanted with WT or TTP$^{-/-}$ bone marrow cells and fed Western diet for 12 weeks and subjected to Affymetrix microarray analysis. N = 4/group. (A) Heat maps of 236 genes that are significantly changed by more than 2 folds and corrected P-value cut-off:0.05. See Supplementary Fig. S6 for detailed gene list. (B) Heat maps of 27 hepatic genes involved in inflammation and lipid metabolism. Color-coding indicates increased gene expressions in red and decreased gene expressions in green. The columns and rows in the heat maps represent samples and genes, respectively. (C) The network in the ingenuity pathway analysis (IPA) from top regulated pathway "inflammatory response" were shown. Genes that are significantly upregulated by bone marrow TTP deficiency are boxed. The color intensity indicates the fold change expression of genes (red representing upregulation and green representing downregulation). (D) The network in the IPA from top regulated pathway "Fatty acid metabolism" were shown. Gene that is significantly downregulated by bone marrow TTP deficiency is boxed. The color intensity indicates the fold change expression of genes (red representing upregulation and green representing downregulation). (E) qPCR analysis of liver mRNA was used to verify the results of selected genes from microarray data. Data were presented as the mean ± SEM. *p < 0.05. Microarray data was deposited at NIH-GEO dataset "GEO accession GSE126481". (For interpretation of the references to color in this figure legend, the reader is referred to the Web version of this article.)

atherosclerotic cardiovascular diseases [46–48]. TTP has been shown to regulate oxidative stress in yeast as TTP overexpression decreased ROS production and mitochondrial membrane potential whereas deletion of TTP significantly increased mitochondrial membrane potential [49]. However, whether TTP deficiency increased mitochondrial ROS production in a murine model of atherosclerosis have not been studied. Therefore, we compared our BM-TTP$^{-/-}$ differentially expressed genes from our microarray data to the 1158 nuclear DNA–encoded mitochondrial genes from Mouse MitoCarta website (https://www.broadinstitute.org/files/shared/metabolism/mitocarta/mouse.mitocarta2.0.html). We found that four out of 236 genes from BM TTP$^{-/-}$ significantly changed genes were related to mitochondrial biology function including Cox8b, Hao2, Abcd1, and Nt5dc2 (Fig. 5A). Accumulative evidence showed that deficiency of Abcd1 was associated with increased oxidative stress and mitochondrial ROS production [50,51]. Our microarray data showed that Abcd1 was significantly downregulated (fold change 2.2) with BM TTP deficiency. Therefore, we examined the mitochondrial ROS production in bone marrow derived macrophages isolated from TTP$^{-/-}$ and littermate control mice after stimulation with hydrogen peroxide. Indeed, we found that TTP deficiency dramatically increased macrophage mitochondrial ROS production after stimulation with H_2O_2 (Fig. 5B). Collectively, these data indicated that as an important mechanism, bone marrow TTP deficiency not only modulates the expressions of oxidative stress genes

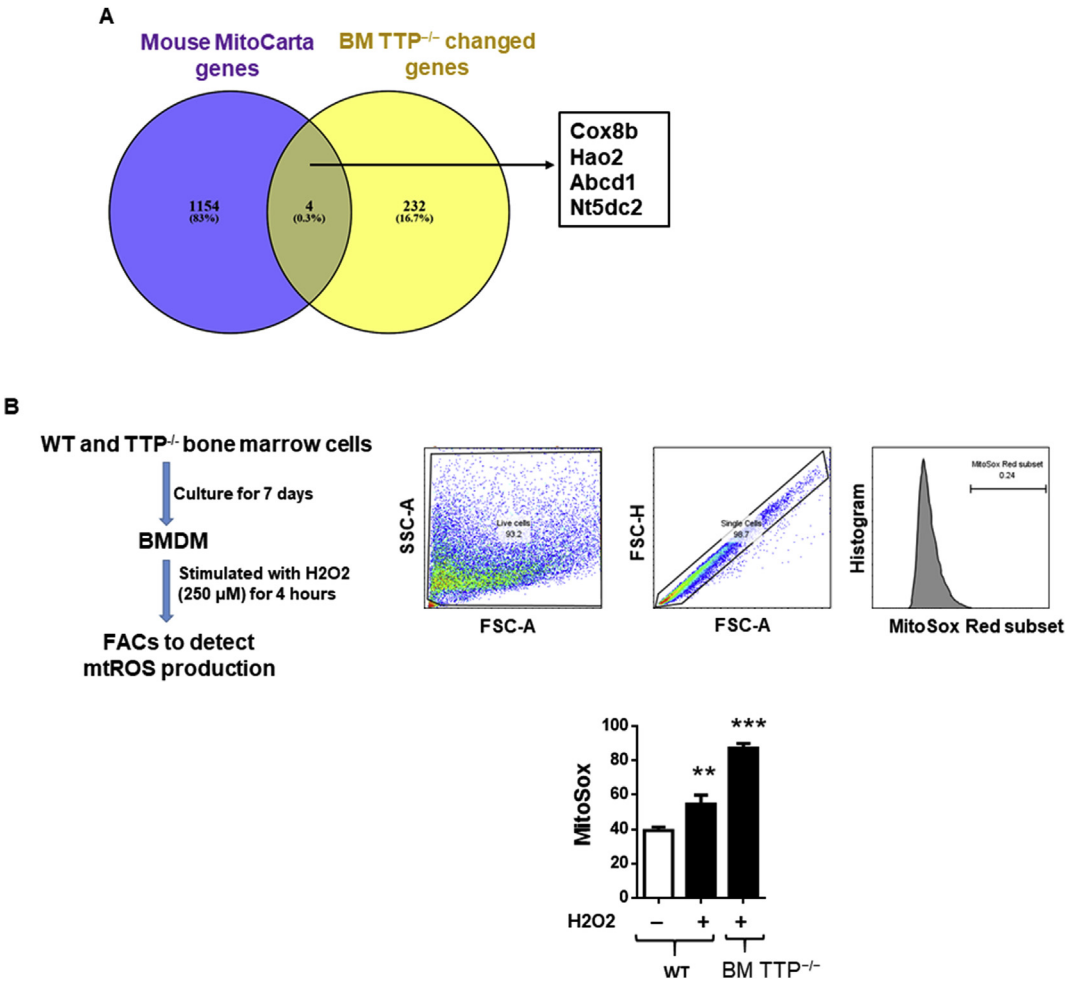

Fig. 5. Bone marrow TTP deficiency increased mitochondrial reactive oxygen species (mtROS) generation. (A) Venn diagram showed some of the mitochondrial biology related genes from mouse mitocarta gene list which is significantly changed in BM $TTP^{-/-}$ mice based on the microarray data. The mitocarta gene list was collected from the MIT Broad Institute website which includes all the nucleus and DNA encoded mitochondrial genes. (B) Mitochondrial ROS production. BMDMs were generated from bone marrow cells isolated from femurs and tibias of $TTP^{-/-}$ mice and WT littermates. Then, cells were treated with H_2O_2 (250 μM) for 4 h, then loaded with 5 μM of MitoSOX Red Mitochondrial Superoxide indicator (Life technologies) for 20 min and flow cytometry analysis was performed to quantify mtROS (n = 3). **P < 0.01; ***P < 0.001, vs. control. (For interpretation of the references to color in this figure legend, the reader is referred to the Web version of this article.)

and nuclear DNA-encoded mitochondrial genes (mitoCarta gene list), but also increases mtROS production.

3.8. Bone marrow TTP deficiency reduces serum lipid levels, alleviates hepatic steatosis, and reduces cholesterol excretion

To corroborate the microarray gene expression data, we analyzed the lipid profile of $LDLR^{-/-}$ mice transplanted with $TTP^{-/-}$ or $TTP^{+/+}$ BM cells. Interestingly, $LDLR^{-/-}$ mice that received $TTP^{-/-}$ BM cells showed a significant reduction in their serum total cholesterol and triglyceride levels after 8 weeks (Supplemental Figs. S4A and S4B) and 12 weeks (Fig. 6A and B) of Western diet feeding, which is consistent with the cachexia and metabolically unhealthy lean phenotype caused by BM TTP deficiency. Fast Protein Liquid Chromatography (FPLC) analyses of serum lipoproteins profile showed a difference in VLDL, LDL, and HDL cholesterol peaks between BM-$TTP^{-/-}$, and BM-$TTP^{+/+}$ $LDLR^{-/-}$ mice. BM-$TTP^{-/-}$ mice exhibited a significant reduction in VLDL/LDL cholesterol levels whereas no significant difference was observed in HDL cholesterol levels (Fig. 6C). Therefore, the VLDL + LDL to HDL cholesterol ratio was significantly reduced by BM TTP deficiency (Fig. 6D), which is consistent with previous human data that showed a significant lower LDL/HDL cholesterol ratio in non-cardiovascular disease individuals than in cardiovascular disease patients [52] (Fig. 6E). We also measured blood glucose levels and body temperature at the experimental end point. There were no differences in blood glucose levels (Supplemental Fig. S5A) and body temperature (Supplemental Fig. S5B) between the groups.

Given the critical role of the liver in lipoprotein and lipid metabolism and the dramatic reduction in plasma lipids and VLDL/LDL cholesterol fractions in BM-$TTP^{-/-}$ mice, we examined lipid accumulation in the liver using Oil Red-O (ORO) staining of fixed liver tissues; and showed that BM TTP deficiency dramatically reduced hepatocyte lipid accumulation (Fig. 6F and G). We also measured cholesterol excretion in the feces and found that cholesterol fecal excretion was significantly reduced in BM-$TTP^{-/-}$ mice (Fig. 6H). Collectively, our data suggests that BM TTP deficiency in atherogenic $LDLR^{-/-}$ mice fed a Western diet not only modulates the expression of liver genes involved in inflammation and lipid metabolism but also results in significant reduction of hepatic lipid production, reduces serum VLDL/LDL cholesterol levels, attenuates hepatic steatosis, and reduces cholesterol fecal excretion, which once again demonstrates the functional significance and underlying mechanisms of BM TTP deficiency-induced downregulation of master regulator SREBF1 in liver.

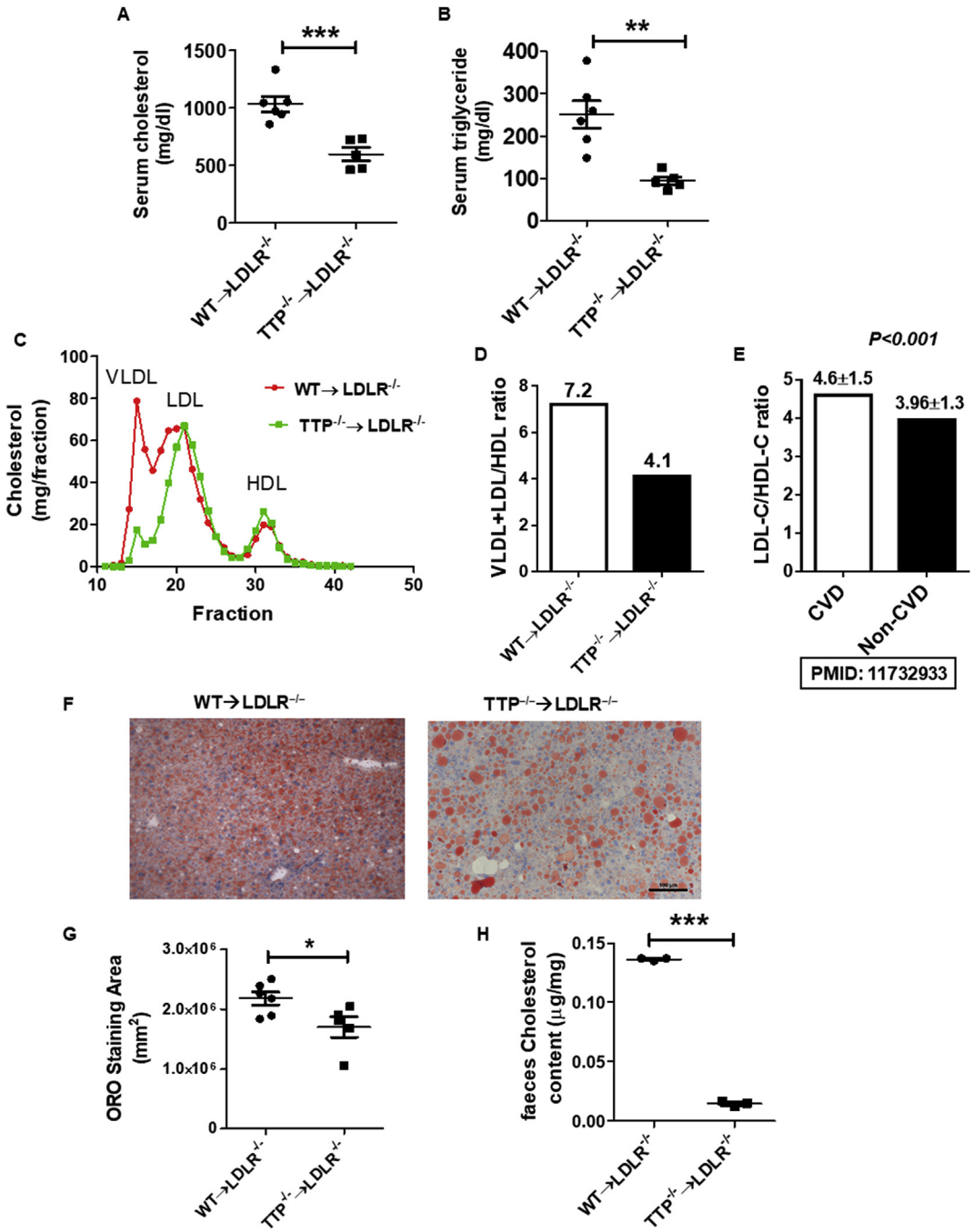

Fig. 6. Bone marrow TTP deficiency reduced serum lipid levels, alleviated hepatic steatosis, and reduced cholesterol excretion. (A) Mouse serum total cholesterol and (B) triglyceride levels were measured after 12 weeks of Western diet. (C) Pooled serum samples from mice at the experimental endpoint were analyzed for the lipoprotein profile using FPLC. Cholesterol content in each fraction was determined (n = 6 mice/group). Data represent the mean ± SEM. (D) Very low density lipoprotein (VLDL) and low density lipoprotein (LDL)/high density lipoprotein (HDL) ratio in BM-TTP$^{-/-}$ mice compared to controls. (E) LDL cholesterol/HDL cholesterol ration in cardiovascular disease (CVD) patient compared to non-CVD individuals. Representative Oil Red-O stained liver sections. Scale bar 100 μm. (F) Quantification of Oil Red-O staining. (G) Fecal cholesterol excretion. *$p < 0.05$; **$p < 0.01$; ***$p < 0.001$. (For interpretation of the references to color in this figure legend, the reader is referred to the Web version of this article.)

3.9. Bone marrow TTP deficiency has no effects on atherogenesis in LDLR$^{-/-}$ mice fed a Western diet

To examine the effects of BM TTP deficiency on atherosclerosis, we analyzed atherosclerosis development in the aortic roots of the BM-TTP$^{-/-}$ LDLR$^{-/-}$ mice after 12 weeks of Western diet feeding. We found that BM TTP deficiency in LDLR$^{-/-}$ mice did not significantly modify the lesion size (Fig. 7A). Similarly, there were no differences in lipid contents (Fig. 7B), macrophage content (Fig. 7C), or collagen percentage (Fig. 7D) in the aortic root, compared with the control mice. These data indicate that the atherogenic effects of BM TTP deficiency on inflammation and the anti-atherogenic effects on liver lipoprotein metabolism may offset each other, leading to unchanged atherosclerosis in LDLR$^{-/-}$ mice fed a Western diet.

4. Discussion

There are two major pathogenic thrusts that drive the atherogenic

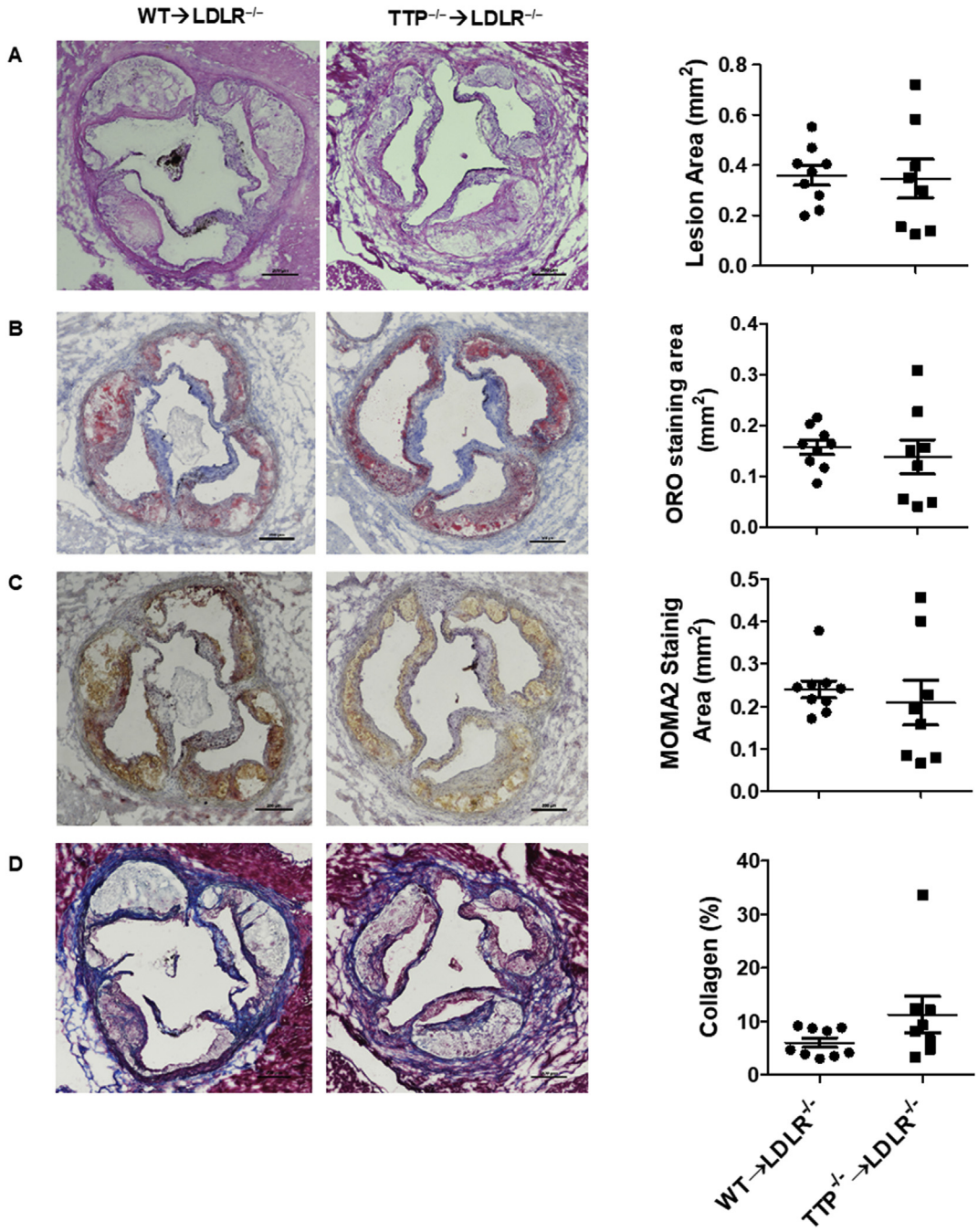

Fig. 7. Bone marrow TTP deficiency had no effects on atherosclerosis after 12 weeks of Western diet feeding in LDLR$^{-/-}$ mice. (A) The lesion area of the frozen sections were detected by H&E staining and quantified by Image-ProPlus 6.0. The quantitative analysis and representative images are shown. (b) Lipid contents in the aortic lesions were determined by ORO staining. Quantitative analysis and representative images are shown. (C) The areas of macrophages in the aortic root lesions were determined by immunostaining for MOMA-2 (a macrophage marker). Quantitative analysis and representative images are shown. (D) Collagen percentage in the aortic root lesions were determined by trichrome staining. Quantitative analysis and representative images are shown. Data were presented as the mean ± SEM (N = 9 mice per group). Scale bar 100 μm.

process: 1) dyslipidemia affecting each of the lipoprotein fractions, and 2) inflammatory responses. These two components are not unrelated as accumulating evidence indicates the cross talk between the immune response and lipid metabolism in the context of atherosclerotic cardiovascular diseases. These interactions have been widely studied and data have shown that lipid accumulation induces macrophage inflammation within the atherosclerotic lesions [53,54]. In addition, cholesterol accumulation in early atherosclerosis has been shown to induce inflammasome/caspase-1 activation, increased IL-1β secretion, and is thus considered as a novel initiator of inflammation [55].

TTP has been shown to be expressed in vascular endothelial cells overlying atherosclerotic lesions in mice and humans and has been reported to play a significant role in controlling vascular inflammation through a direct binding to target cytokine/chemokine mRNAs [33]. TNFalpha is the best-known pathophysiological target of TTP [8]. TNFalpha is a key determinant for inflammation as it is usually one of the first responders in the inflammatory pathway [56]. Mice with a genetic disruption of TTP display severe inflammatory syndrome due to overproduction of TNFalpha; and TNFalpha antibody treatment or TNFalpha receptor deficiency could attenuate development of the

inflammatory phenotype associated with TTP deficiency [8,17]. More importantly, TTP$^{-/-}$ mice crossed into apoE$^{-/-}$ mice and fed a normal chow diet show more aortic atherosclerotic lesions than apoE$^{-/-}$ mice; however, TTP$^{-/-}$/apoE$^{-/-}$ mice showed a reduction in their total cholesterol and triglyceride levels indicating that TTP may play a critical role in regulating lipid metabolism during atherogenesis [57]. However, the roles of TTP in bone marrow-derived cells on modulating lipid metabolism and atherosclerosis have never been examined, which we studied thoroughly using BM TTP deficiency in LDLR$^{-/-}$ mice fed a Western diet.

Although both inflammation and dyslipidemia are key risk factors for atherosclerotic cardiovascular diseases, it is still incompletely understood regarding to their relative contribution to atherosclerosis, since in almost all atherogenic animal models, hyperlipidemia is accompanied with increased inflammation. We set out to address this issue in this study. First, we measured TTP expression in human carotid atherosclerotic lesions; and then we performed a bone marrow transplantation study to determine how TTP deficiency in bone marrow-derived cells impacts atherogenesis in LDLR$^{-/-}$ mice fed a Western diet. By performing hematological, histological, flow cytometry, biochemical, metabolic, and microarray analyses, we were able to demonstrate the following exciting findings: *1)* TTP mRNA level was slightly, but statistically significantly, up-regulated in human carotid atherosclerotic lesions compared to the surrounding normal tissue of the same CEA patients, suggesting that TTP may play a regulatory role during the atherogenic process; *2)* BM TTP deficiency in LDLR$^{-/-}$ mice resulted in increased pro-inflammatory cytokine secretion from LPS stimulated peritoneal macrophages, suggesting that deletion of TTP in bone marrow cells increased responsiveness of macrophages to LPS stimulation; *3)* BM-TTP$^{-/-}$ mice displayed select hematopoietic and immunological abnormalities including increased neutrophil granulocytes, platelet count, and platelet hematocrit in the peripheral blood; *4)* BM TTP deficiency in LDLR$^{-/-}$ mice resulted in reduced body weight, mirroring a metabolically unhealthy lean phenotype; *5)* BM TTP deficiency in LDLR$^{-/-}$ mice resulted in upregulation of inflammatory TNFalpha and increased inflammatory cell infiltration in various organs, suggesting that hematopoietic progenitors are responsible for the development of the inflammatory syndrome; *6)* BM TTP deficiency in LDLR$^{-/-}$ mice resulted in altered expression of both inflammatory genes and lipid related genes in the liver; of note, the expression SREBF1, a key transcription factor regulating lipogenic enzymes, was shown to be downregulated by BM TTP deficiency; *7)* BM TTP deficiency significantly increased mitochondrial ROS production in H_2O_2 stimulated BMDM;*8)* BM TTP deficiency dramatically reduced serum total cholesterol and triglyceride levels in LDLR$^{-/-}$ mice after consumption of a Western diet. Interestingly, VLDL cholesterol, which is mostly produced by the liver, was most drastically reduced by BM TTP deficiency, suggesting that reduced serum total cholesterol and triglyceride levels result from reduced hepatic lipid production due to downregulation of the SREBF1 gene; *9)* BM TTP deficiency attenuated hepatic steatosis and fecal cholesterol excretion; and *10)* BM TTP deficiency did not significantly affect Western diet-induced atherosclerotic lesion development in LDLR$^{-/-}$ mice, suggesting that reduced lipoprotein production may offset the effects of the concomitant increase in inflammation. These results suggest the followings: *First*, in a normal situation, TTP promotes TNFalpha mRNA degradation; therefore, TTP deficiency will stabilize and increase TNFalpha secretion leading to a pro-inflammatory status. *Second*, TTP can indirectly promote VLDL/LDL biosynthesis by its potential to cause destabilization and degradation of the mRNA of the upstream negative regulators of VLDL/LDL biosynthesis, such as insulin induced gene 1(INSIG1), which blocks SREBF1 from acting as a transcription factor in the promoter region of the HMG-CoA reductase gene and results in a decreased expression of HMG-CoA reductase [58]. Therefore, TTP deficiency results in stabilization of the upstream negative regulators and consequently inhibits VLDL/LDL biosynthesis enzymes and reduces VLDL/LDL levels. *Third*, TTP can promote VLDL/LDL biosynthesis directly by potentially stabilizing the mRNA of VLDL/LDL biosynthesis enzymes such as HMG-CoA reductase or SREBF1 transcription factor; therefore, as our results suggest, TTP deficiency leads to reduced SREBF1 and decreased VLDL/LDL biosynthesis. By default, many AU-rich elements (AREs) destabilize and repress mRNA translation; however, they also can respond to inflammatory stimuli, by stabilizing the mRNA and de-repressing its translation [6,59].

The roles of inflammation and lipid metabolism in atherosclerosis development have been extensively studied, but their relative contribution remains elusive. A relationship exists between LDL cholesterol levels in the circulation and inflammatory responses that promote atherosclerosis. Increased LDL cholesterol levels are strongly correlated with risk of atherosclerosis development in humans and with circulating markers of inflammation [60]. However, despite these clear relationships, how these two major components are intertwined in the development of hyperlipidemic cardiovascular diseases and the underlying molecular mechanisms remain incompletely understood.

BMT has been widely used to examine the role of leukocyte gene expression in atherogenesis through modulating inflammation or lipid metabolism [61–64]; however, none of these studies have shown that BMT can influence both lipid metabolism and inflammation concomitantly. The effect of transplantation of TTP$^{-/-}$ bone marrow cells into LDLR$^{-/-}$ mice fed a Western diet on inflammation and lipid metabolism during atherogenic process were simultaneously examined in our study. Previous reports showed that SREBF1 transcriptionally increased lipogenic genes and regulated liver *de novo* lipogenesis [65]. Moreover, human data showed that increased SREBF1 levels correlated with hepatic steatosis [66]; and that SREBF1 knockdown reduces hepatic *de novo* lipogenesis and steatosis [67]. Another study showed that hepatic SREBF1 overexpression in LDLR$^{-/-}$ mice results in increased serum lipid, VLDL cholesterol, and accelerated atherosclerosis whereas systemic SREBF1 deficiency dramatically reduces plasma lipid, VLDL cholesterol, and reduces atherosclerotic lesion formation in LDLR$^{-/-}$ mice fed a Western diet [68]. Furthermore, it has been reported that increased oxidative stress and downregulated anti-oxidative pathways accelerated inflammation and inhibited *de novo* lipogenesis with the suppression of SREBF1 [69]. Our results show that BM TTP deficiency significantly reduced hepatic SREBF1 expression and thus VLDL/LDL cholesterol, leading to reduced plasma lipid levels and attenuated hepatic steatosis. Also, BM TTP deficiency and TTP target gene SREBF1 modulated oxidative regulator expression. MicroRNA-27a (miR-27a) is a pro-inflammatory miRNA expressed in the macrophages [70] and can be circulated in exosomes [71]. MiRNAs can be secreted from cells including macrophages into the extracellular space within the exosomes [72]. These cell-derived exosomes contain numerous miRNAs, which can be taken up into neighboring or distant cell types including hepatocytes to modulate their function [73]. Moreover, previous studies demonstrated that miR-27a can interacts with the HMG-CoA reductase 3′ untranslated region in murine and human hepatocytes and downregulate its expression [74]. Therefore, we believe that the miR-27a within the exosomes presumably secreted from TTP deficient bone marrow derived macrophages as the exosome dock on the hepatocyte modulate the hepatocyte lipid metabolism and downregulate the HMG-CoA reductase mRNA. Therefore, we believe this could be a potential mechanism for TTP deficient bone marrow derived macrophage in modulating hepatic cell lipid metabolism. Of note, the future studies are warranted to determine the novel molecular mechanisms underlying the regulation of TTP deficient bone marrow-derived cells on hepatic, and other tissue expressions of SREBF1 and other lipid metabolism regulators and inflammation regulators.

Based on our findings, we propose a working model for TTP as illustrated in Fig. 8: *1)* Under normal physiological conditions, TTP inhibits inflammation through the degradation of TNFalpha mRNA transcripts and potentially other pro-inflammatory cytokine mRNAs, leading to an anti-inflammatory status, which presumably suppress pro-

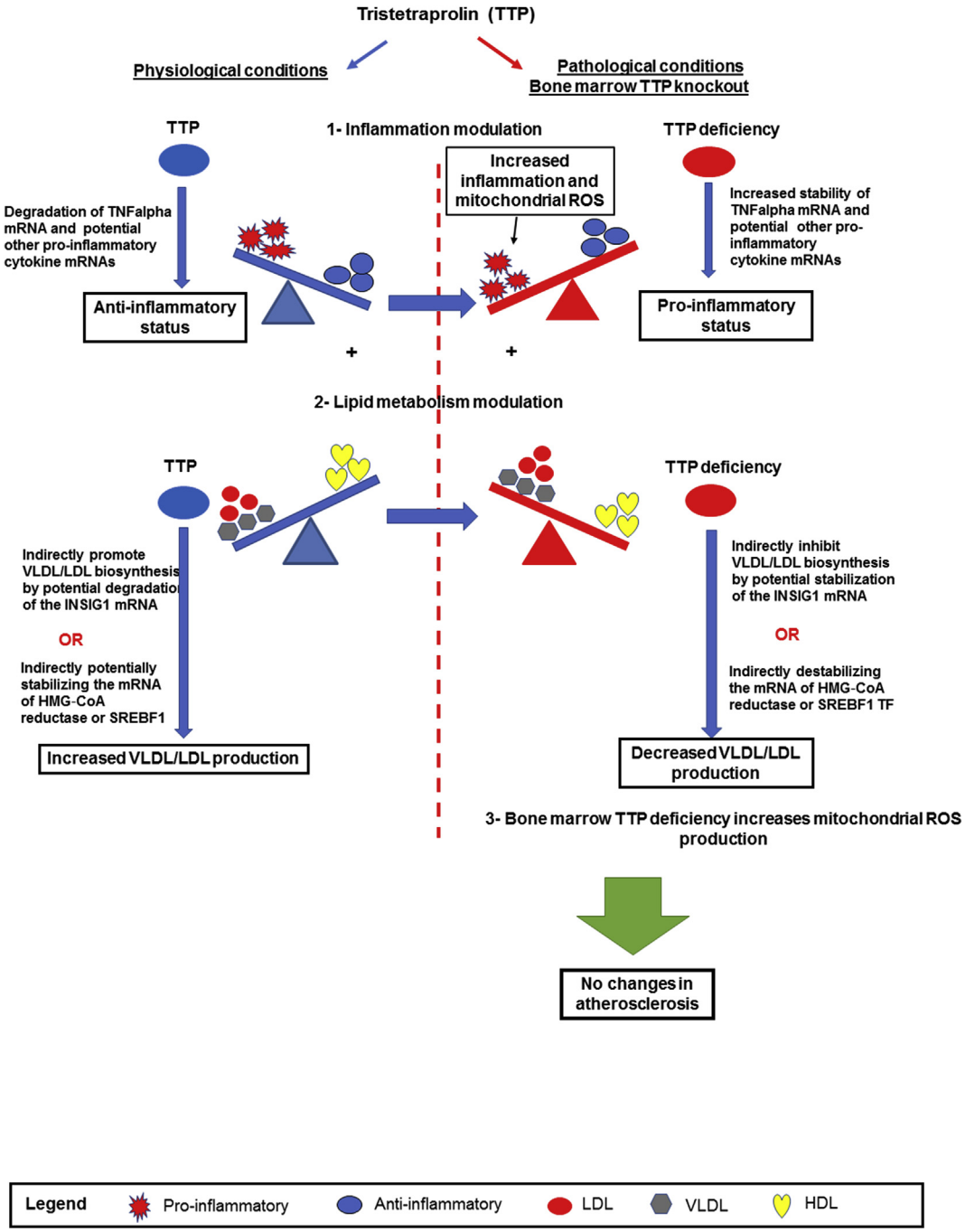

Fig. 8. Schematic representation of a working model. TTP modulates both inflammation and lipid metabolism. Left: During normal physiological condition, TTP acts as an anti-inflammatory molecule by degrading pro-inflammatory TNFalpha mRNA and potentially other pro-inflammatory cytokine mRNAs. Concurrently, TTP increases VLDL/LDL cholesterol indirectly by degrading negative up-regulator INSIG1 mRNA or indirectly by stabilizing HMG-CoA reductase/SREBF1 mRNAs. Right: under pathological conditions, bone marrow TTP deficiency in LDLR$^{-/-}$ mice increased inflammation by stabilizing TNFalpha mRNA and potential other pro-inflammatory cytokine mRNAs and increasing mtROS production. At the same, TTP deficiency indirectly decreases VLDL/LDL cholesterol by potentially stabilizing the insulin induced gene 1 (INSIG1) mRNA or indirectly by destabilizing the mRNA of HMG-CoA reductase or SREBF1 mRNAs. Increased inflammation, mtROS, and reduced lipids offsets each other, resulting in unchanged atherosclerosis in BM TTP deficient mice.

inflammatory potential derived from lipid metabolism; *2)* At the same time, TTP can modulate pro-inflammatory lipid metabolism by promoting VLDL/LDL biosynthesis indirectly via degradation of the negative upstream regulator of VLDL/LDL biosynthesis such as INSIG-1 mRNA or indirectly by stabilizing HMG-CoA reductase or SREBF1 mRNAs; *3)* BM TTP deficiency results in increased pro-inflammatory status through stabilization of TNFalpha and potential other pro-inflammatory cytokine mRNAs and increase of ROS promoter expressions and mitochondrial ROS; and 4) Concomitantly, TTP deficiency in bone marrow decreases VLDL/LDL biosynthesis indirectly by stabilization of INSIG-1 mRNA or indirectly by destabilizing the mRNA of HMG-CoA reductase or SREBF1. Increased inflammation and reduced VLDL/LDL production offset each other, resulting in unchanged atherosclerosis. While more detailed molecular mechanisms in these regards warrant further investigation, our findings provide a novel insight into how general mRNA decaying proteins can modulate multiple pathological pathways in the context of atherogenesis. In summary, our study identified the roles of TTP-mediated mRNA decay in bone marrow-

derived cells in regulating systemic inflammation and hepatic lipid metabolism. Since lipid metabolism and inflammation play roles in many diseases such as cardiovascular diseases, metabolic diseases and cancers, TTP may serve as a molecular target in the treatment or prevention of these diseases.

Source of funding

This work was supported by NIH grants R01HL116626 (to DF) and 1R01 HL138749-01 (XY), and was also supported in part by the Intramural Research Program of the National Institute of Environmental Health Sciences, NIH (to PJB).

Declaration of competing interest

No potential conflicts of interest were disclosed.

Appendix A. Supplementary data

Supplementary data to this article can be found online at https://doi.org/10.1016/j.redox.2020.101609.

References

[1] S.A. Brooks, P.J. Blackshear, Tristetraprolin (ttp): interactions with mrna and proteins, and current thoughts on mechanisms of action, Biochim. Biophys. Acta 1829 (2013) 666–679.
[2] P.J. Blackshear, Tristetraprolin and other ccch tandem zinc-finger proteins in the regulation of mrna turnover, Biochem. Soc. Trans. 30 (2002) 945–952.
[3] L. Ramos-Alonso, A.M. Romero, J. Polaina, S. Puig, M.T. Martinez-Pastor, Dissecting mrna decay and translation inhibition during iron deficiency, Curr. Genet. 65 (2019) 139–145.
[4] S. Patial, P.J. Blackshear, Tristetraprolin as a therapeutic target in inflammatory disease, Trends Pharmacol. Sci. 37 (2016) 811–821.
[5] W.S. Lai, E. Carballo, J.R. Strum, E.A. Kennington, R.S. Phillips, P.J. Blackshear, Evidence that tristetraprolin binds to au-rich elements and promotes the deadenylation and destabilization of tumor necrosis factor alpha mrna, Mol. Cell Biol. 19 (1999) 4311–4323.
[6] D.R. Schoenberg, L.E. Maquat, Regulation of cytoplasmic mrna decay, Nat. Rev. Genet. 13 (2012) 246–259.
[7] E. Carballo, W.S. Lai, P.J. Blackshear, Feedback inhibition of macrophage tumor necrosis factor-alpha production by tristetraprolin, Science 281 (1998) 1001–1005.
[8] G.A. Taylor, E. Carballo, D.M. Lee, W.S. Lai, M.J. Thompson, D.D. Patel, et al., A pathogenetic role for tnf alpha in the syndrome of cachexia, arthritis, and autoimmunity resulting from tristetraprolin (ttp) deficiency, Immunity 4 (1996) 445–454.
[9] E. Carballo, W.S. Lai, P.J. Blackshear, Evidence that tristetraprolin is a physiological regulator of granulocyte-macrophage colony-stimulating factor messenger rna deadenylation and stability, Blood 95 (2000) 1891–1899.
[10] R.L. Ogilvie, M. Abelson, H.H. Hau, I. Vlasova, P.J. Blackshear, P.R. Bohjanen, Tristetraprolin down-regulates il-2 gene expression through au-rich element-mediated mrna decay, J. Immunol. 174 (2005) 953–961.
[11] G. Stoecklin, X.F. Ming, R. Looser, C. Moroni, Somatic mrna turnover mutants implicate tristetraprolin in the interleukin-3 mrna degradation pathway, Mol. Cell Biol. 20 (2000) 3753–3763.
[12] G. Stoecklin, S.A. Tenenbaum, T. Mayo, S.V. Chittur, A.D. George, T.E. Baroni, et al., Genome-wide analysis identifies interleukin-10 mrna as target of tristetraprolin, J. Biol. Chem. 283 (2008) 11689–11699.
[13] L. Gu, H. Ning, X. Qian, Q. Huang, R. Hou, R. Almourani, et al., Suppression of il-12 production by tristetraprolin through blocking nf-kcyb nuclear translocation, J. Immunol. 191 (2013) 3922–3930.
[14] K. Deng, H. Wang, T. Shan, Y. Chen, H. Zhou, Q. Zhao, et al., Tristetraprolin inhibits gastric cancer progression through suppression of il-33, Sci. Rep. 6 (2016) 24505.
[15] R.L. Ogilvie, J.R. Sternjohn, B. Rattenbacher, I.A. Vlasova, D.A. Williams, H.H. Hau, et al., Tristetraprolin mediates interferon-gamma mrna decay, J. Biol. Chem. 284 (2009) 11216–11223.
[16] D.M. Carrick, W.S. Lai, P.J. Blackshear, The tandem ccch zinc finger protein tristetraprolin and its relevance to cytokine mrna turnover and arthritis, Arthritis Res. Ther. 6 (2004) 248–264.
[17] E. Carballo, P.J. Blackshear, Roles of tumor necrosis factor-alpha receptor subtypes in the pathogenesis of the tristetraprolin-deficiency syndrome, Blood 98 (2001) 2389–2395.
[18] F. Bollmann, Z. Wu, M. Oelze, D. Siuda, N. Xia, J. Henke, et al., Endothelial dysfunction in tristetraprolin-deficient mice is not caused by enhanced tumor necrosis factor-alpha expression, J. Biol. Chem. 289 (2014) 15653–15665.
[19] F.R. Ponziani, S. Pecere, A. Gasbarrini, V. Ojetti, Physiology and pathophysiology of liver lipid metabolism, Expet Rev. Gastroenterol. Hepatol. 9 (2015) 1055–1067.
[20] E. Galkina, K. Ley, Immune and inflammatory mechanisms of atherosclerosis (*), Annu. Rev. Immunol. 27 (2009) 165–197.
[21] G.K. Hansson, P. Libby, The immune response in atherosclerosis: a double-edged sword, Nat. Rev. Immunol. 6 (2006) 508–519.
[22] M. Jan, S. Meng, N.C. Chen, J. Mai, H. Wang, X.F. Yang, Inflammatory and autoimmune reactions in atherosclerosis and vaccine design informatics, J. Biomed. Biotechnol. 2010 (2010) 459798.
[23] L. Jonasson, J. Holm, O. Skalli, G. Bondjers, G.K. Hansson, Regional accumulations of t cells, macrophages, and smooth muscle cells in the human atherosclerotic plaque, Arteriosclerosis 6 (1986) 131–138.
[24] P. Libby, P.M. Ridker, G.K. Hansson, Progress and challenges in translating the biology of atherosclerosis, Nature 473 (2011) 317–325.
[25] I. Vukovic, N. Arsenijevic, V. Lackovic, V. Todorovic, The origin and differentiation potential of smooth muscle cells in coronary atherosclerosis, Exp. Clin. Cardiol. 11 (2006) 123–128.
[26] K.J. Woollard, F. Geissmann, Monocytes in atherosclerosis: subsets and functions, Nat. Rev. Cardiol. 7 (2010) 77–86.
[27] R. Ross, L. Harker, Hyperlipidemia and atherosclerosis, Science 193 (1976) 1094–1100.
[28] P. Libby, Inflammation in atherosclerosis, Arterioscler. Thromb. Vasc. Biol. 32 (2012) 2045–2051.
[29] K.J. Moore, F.J. Sheedy, E.A. Fisher, Macrophages in atherosclerosis: a dynamic balance, Nat. Rev. Immunol. 13 (2013) 709–721.
[30] P.M. Ridker, B.M. Everett, T. Thuren, J.G. MacFadyen, W.H. Chang, C. Ballantyne, et al., Antiinflammatory therapy with canakinumab for atherosclerotic disease, N. Engl. J. Med. 377 (2017) 1119–1131.
[31] P.M. Ridker, E. Danielson, F.A. Fonseca, J. Genest, A.M. Gotto Jr., J.J. Kastelein, et al., Rosuvastatin to prevent vascular events in men and women with elevated c-reactive protein, N. Engl. J. Med. 359 (2008) 2195–2207.
[32] J. Weischenfeldt, B. Porse, Bone marrow-derived macrophages (bmm): isolation and applications, CSH Protocols (2008), https://doi.org/10.1101/pdb.prot5080 2008:pdb.prot5080. Published 2008 Dec 1.
[33] H. Zhang, W.R. Taylor, G. Joseph, V. Caracciolo, D.M. Gonzales, N. Sidell, et al., Mrna-binding protein zfp36 is expressed in atherosclerotic lesions and reduces inflammation in aortic endothelial cells, Arterioscler. Thromb. Vasc. Biol. 33 (2013) 1212–1220.
[34] W.D. Patino, J.G. Kang, S. Matoba, O.Y. Mian, B.R. Gochuico, P.M. Hwang, Atherosclerotic plaque macrophage transcriptional regulators are expressed in blood and modulated by tristetraprolin, Circ. Res. 98 (2006) 1282–1289.
[35] E. Carballo, G.S. Gilkeson, P.J. Blackshear, Bone marrow transplantation reproduces the tristetraprolin-deficiency syndrome in recombination activating gene-2 (-/-) mice. Evidence that monocyte/macrophage progenitors may be responsible for TNFalpha overproduction, J. Clin. Invest. 100 (1997) 986–995.
[36] I.M. Kaplan, S. Morisot, D. Heiser, W.C. Cheng, M.J. Kim, C.I. Civin, Deletion of tristetraprolin caused spontaneous reactive granulopoiesis by a non-cell-autonomous mechanism without disturbing long-term hematopoietic stem cell quiescence, J. Immunol. 186 (2011) 2826–2834.
[37] H. Huang, A. Fletcher, Y. Niu, T.T. Wang, L. Yu, Characterization of lipopolysaccharide-stimulated cytokine expression in macrophages and monocytes, Inflamm. Res. 61 (2012) 1329–1338.
[38] E.A. Kaperonis, C.D. Liapis, J.D. Kakisis, D. Dimitroulis, V.G. Papavassiliou, Inflammation and atherosclerosis, Eur. J. Vasc. Endovasc. Surg. 31 (2006) 386–393.
[39] Y. Wang, J. Viscarra, S.J. Kim, H.S. Sul, Transcriptional regulation of hepatic lipogenesis, Nat. Rev. Mol. Cell Biol. 16 (2015) 678–689.
[40] J. Han, Y. Wang, Mtorc1 signaling in hepatic lipid metabolism, Protein Cell 9 (2018) 145–151.
[41] G. Musso, R. Gambino, M. Cassader, Recent insights into hepatic lipid metabolism in non-alcoholic fatty liver disease (nafld), Prog. Lipid Res. 48 (2009) 1–26.
[42] M.T. Bengoechea-Alonso, J. Ericsson, Srebp in signal transduction: cholesterol metabolism and beyond, Curr. Opin. Cell Biol. 19 (2007) 215–222.
[43] S.C. de Jager, G. Pasterkamp, Crosstalk of lipids and inflammation in atherosclerosis: the pro of pgrn? Cardiovasc. Res. 100 (2013) 4–6.
[44] T. Finkel, N.J. Holbrook, Oxidants, oxidative stress and the biology of ageing, Nature 408 (2000) 239–247.
[45] P.S. Hartman, N. Ishii, E.B. Kayser, P.G. Morgan, M.M. Sedensky, Mitochondrial mutations differentially affect aging, mutability and anesthetic sensitivity in caenorhabditis elegans, Mech. Ageing Dev. 122 (2001) 1187–1201.
[46] X. Li, P. Fang, J. Mai, E.T. Choi, H. Wang, X.F. Yang, Targeting mitochondrial reactive oxygen species as novel therapy for inflammatory diseases and cancers, J. Hematol. Oncol. 6 (2013) 19.
[47] X. Li, P. Fang, Y. Li, Y.M. Kuo, A.J. Andrews, G. Nanayakkara, et al., Mitochondrial reactive oxygen species mediate lysophosphatidylcholine-induced endothelial cell activation, Arterioscler. Thromb. Vasc. Biol. 36 (2016) 1090–1100.
[48] X. Li, Y. Shao, X. Sha, P. Fang, Y.M. Kuo, A.J. Andrews, et al., Il-35 (interleukin-35) suppresses endothelial cell activation by inhibiting mitochondrial reactive oxygen species-mediated site-specific acetylation of h3k14 (histone 3 lysine 14), Arterioscler. Thromb. Vasc. Biol. 38 (2018) 599–609.
[49] R. Matsuo, S. Mizobuchi, M. Nakashima, K. Miki, D. Ayusawa, M. Fujii, Central roles of iron in the regulation of oxidative stress in the yeast saccharomyces cerevisiae, Curr. Genet. 63 (2017) 895–907.
[50] M. Baarine, P. Andreoletti, A. Athias, T. Nury, A. Zarrouk, K. Ragot, et al., Evidence of oxidative stress in very long chain fatty acid–treated oligodendrocytes and potentialization of ros production using rna interference-directed knockdown of abcd1 and acox1 peroxisomal proteins, Neuroscience 213 (2012) 1–18.
[51] S. Fourcade, I. Ferrer, A. Pujol, Oxidative stress, mitochondrial and proteostasis malfunction in adrenoleukodystrophy: a paradigm for axonal degeneration, Free Radic. Biol. Med. 88 (2015) 18–29.

[52] I. Lemieux, B. Lamarche, C. Couillard, A. Pascot, B. Cantin, J. Bergeron, et al., Total cholesterol/hdl cholesterol ratio vs ldl cholesterol/hdl cholesterol ratio as indices of ischemic heart disease risk in men: the quebec cardiovascular study, Arch. Intern. Med. 161 (2001) 2685–2692.
[53] R. Ross, Atherosclerosis–an inflammatory disease, N. Engl. J. Med. 340 (1999) 115–126.
[54] A. Kadl, A.K. Meher, P.R. Sharma, M.Y. Lee, A.C. Doran, S.R. Johnstone, et al., Identification of a novel macrophage phenotype that develops in response to atherogenic phospholipids via nrf2, Circ. Res. 107 (2010) 737–746.
[55] P. Duewell, H. Kono, K.J. Rayner, C.M. Sirois, G. Vladimer, F.G. Bauernfeind, et al., Nlrp3 inflammasomes are required for atherogenesis and activated by cholesterol crystals, Nature 464 (2010) 1357–1361.
[56] V. Baud, M. Karin, Signal transduction by tumor necrosis factor and its relatives, Trends Cell Biol. 11 (2001) 372–377.
[57] J.G. Kang, M.J. Amar, A.T. Remaley, J. Kwon, P.J. Blackshear, P.Y. Wang, et al., Zinc finger protein tristetraprolin interacts with ccl3 mrna and regulates tissue inflammation, J. Immunol. 187 (2011) 2696–2701.
[58] N. Sever, T. Yang, M.S. Brown, J.L. Goldstein, R.A. DeBose-Boyd, Accelerated degradation of hmg coa reductase mediated by binding of insig-1 to its sterol-sensing domain, Mol. Cell. 11 (2003) 25–33.
[59] J. Schott, S. Reitter, J. Philipp, K. Haneke, H. Schafer, G. Stoecklin, Translational regulation of specific mrnas controls feedback inhibition and survival during macrophage activation, PLoS Genet. 10 (2014) e1004368.
[60] G.K. Hansson, A.K. Robertson, C. Soderberg-Naucler, Inflammation and atherosclerosis, Annu. Rev. Pathol. 1 (2006) 297–329.
[61] E.J. Dann, Y. Friedlander, E. Leitersdorf, A. Nagler, The modulation of plasma lipids and lipoproteins during bone marrow transplantation is unrelated to exogenously administered recombinant human granulocyte-monocyte colony-stimulating factor (rhu gm-csf), Med. Oncol. 13 (1996) 81–86.
[62] S. Fazio, M.F. Linton, Murine bone marrow transplantation as a novel approach to studying the role of macrophages in lipoprotein metabolism and atherogenesis, Trends Cardiovasc. Med. 6 (1996) 58–65.
[63] M. Van Eck, N. Herijgers, J. Yates, N.J. Pearce, P.M. Hoogerbrugge, P.H. Groot, et al., Bone marrow transplantation in apolipoprotein e-deficient mice. Effect of apoe gene dosage on serum lipid concentrations, (beta)vldl catabolism, and atherosclerosis, Arterioscler. Thromb. Vasc. Biol. 17 (1997) 3117–3126.
[64] M.T. Bejar, R. Hernandez-Vera, G. Vilahur, L. Badimon, Bone marrow cell transplant from donors with cardiovascular risk factors increases the pro-atherosclerotic phenotype in the recipients, Am. J. Transplant. 16 (2016) 3392–3403.
[65] J.D. Horton, J.L. Goldstein, M.S. Brown, Srebps: activators of the complete program of cholesterol and fatty acid synthesis in the liver, J. Clin. Invest. 109 (2002) 1125–1131.
[66] P. Pettinelli, T. Del Pozo, J. Araya, R. Rodrigo, A.V. Araya, G. Smok, et al., Enhancement in liver srebp-1c/ppar-alpha ratio and steatosis in obese patients: correlations with insulin resistance and n-3 long-chain polyunsaturated fatty acid depletion, Biochim. Biophys. Acta 1792 (2009) 1080–1086.
[67] R. Ruiz, V. Jideonwo, M. Ahn, S. Surendran, V.S. Tagliabracci, Y. Hou, et al., Sterol regulatory element-binding protein-1 (srebp-1) is required to regulate glycogen synthesis and gluconeogenic gene expression in mouse liver, J. Biol. Chem. 289 (2014) 5510–5517.
[68] T. Karasawa, A. Takahashi, R. Saito, M. Sekiya, M. Igarashi, H. Iwasaki, et al., Sterol regulatory element-binding protein-1 determines plasma remnant lipoproteins and accelerates atherosclerosis in low-density lipoprotein receptor-deficient mice, Arterioscler. Thromb. Vasc. Biol. 31 (2011) 1788–1795.
[69] Y. Okuno, A. Fukuhara, E. Hashimoto, H. Kobayashi, S. Kobayashi, M. Otsuki, et al., Oxidative stress inhibits healthy adipose expansion through suppression of srebf1-mediated lipogenic pathway, Diabetes 67 (2018) 1113–1127.
[70] G. Curtale, M. Rubino, M. Locati, Micrornas as molecular switches in macrophage activation, Front. Immunol. 10 (2019) 799.
[71] X. Liu, B. Pan, L. Sun, X. Chen, K. Zeng, X. Hu, et al., Circulating exosomal mir-27a and mir-130a act as novel diagnostic and prognostic biomarkers of colorectal cancer, Canc. Epidemiol. Biomark. Prevent. Publ. Am. Assoc. Canc. Res., Cosponsored Am. Soc. Preventive Oncol. 27 (2018) 746–754.
[72] Y. Chen, J.J. Buyel, M.J. Hanssen, F. Siegel, R. Pan, J. Naumann, et al., Exosomal microrna mir-92a concentration in serum reflects human brown fat activity, Nat. Commun. 7 (2016) 11420.
[73] J. Zhang, S. Li, L. Li, M. Li, C. Guo, J. Yao, et al., Exosome and exosomal microrna: trafficking, sorting, and function, Dev. Reprod. Biol. 13 (2015) 17–24.
[74] A.A. Khan, H. Agarwal, S.S. Reddy, V. Arige, B. Natarajan, V. Gupta, et al., Microrna 27a is a key modulator of cholesterol biosynthesis, Mol. Cell Biol. (2020) 40.